Thin Phytoplankton Layers: Characteristics, Mechanisms, and Consequences

William M. Durham and Roman Stocker

Ralph M. Parsons Laboratory, Department of Civil and Environmental Engineering, Massachusetts Institute of Technology, Cambridge, Massachusetts 02139; email: durham@mit.edu, romans@mit.edu

Keywords

trophic hotspot, marine ecology, phytoplankton motility, hydrodynamic shear, turbulent dispersion

Abstract

For over four decades, aggregations of phytoplankton known as thin layers have been observed to harbor large amounts of photosynthetic cells within narrow horizontal bands. Field observations have revealed complex linkages among thin phytoplankton layers, the physical environment, cell behavior, and higher trophic levels. Several mechanisms have been proposed to explain layer formation and persistence, in the face of the homogenizing effect of turbulent dispersion. The challenge ahead is to connect mechanistic hypotheses with field observations to gain better insight on the phenomena that shape layer dynamics. Only through a mechanistic understanding of the relevant biological and physical processes can we begin to predict the effect of thin layers on the ecology of phytoplankton and higher organisms.

1. INTRODUCTION

The distribution of phytoplankton in the ocean is highly heterogeneous, or patchy, over length scales ranging from thousands of kilometers down to a few centimeters. At large scales, heterogeneity is primarily driven by locally enhanced growth rates, favored by mesoscale processes such as nutrient upwelling and front formation (Lévy 2008). At the smallest scales, patchiness likely arises from interactions of plankton with small-scale chemical or hydrodynamic gradients (Durham et al. 2011, Gallager et al. 2004, Seymour et al. 2009, Waters et al. 2003). This pervasive heterogeneity can affect the mean abundance of both phytoplankton and their predators through their nonlinear interaction (Steele 1974) and may contribute to sustaining the high diversity of plankton (Hutchinson 1961) via habitat partitioning (Bracco et al. 2000).

A particularly dramatic form of patchiness occurs when large numbers of photosynthetic microorganisms are found within a small depth interval. These formations are known as thin phytoplankton layers and have received considerable attention from oceanographers and mathematical modelers, recently culminating in an intensive multi-investigator effort, known as the Layered Organization in the Coastal Ocean project, that took place in Monterey Bay, California, during 2005 and 2006 and was reviewed in an editorial by Sullivan et al. (2010b). Thin layers are temporally coherent aggregations of phytoplankton, typically several centimeters to a few meters thick and often extending for kilometers in the horizontal direction (Dekshenieks et al. 2001, Moline et al. 2010). They are widespread in the coastal ocean, with one study in Monterey Bay reporting thin layers occurring up to 87% of the time (Sullivan et al. 2010a). At times, multiple layers comprising distinct phytoplankton species can occupy different depths in the same water column (Rines et al. 2010).

In what was perhaps the first observation of thin phytoplankton layers (**Figure 1a**), Strickland (1968) noted that standard sampling techniques could lead to substantial errors in the measurement of both the depth-integrated chlorophyll abundance and the concentration of chlorophyll at a given
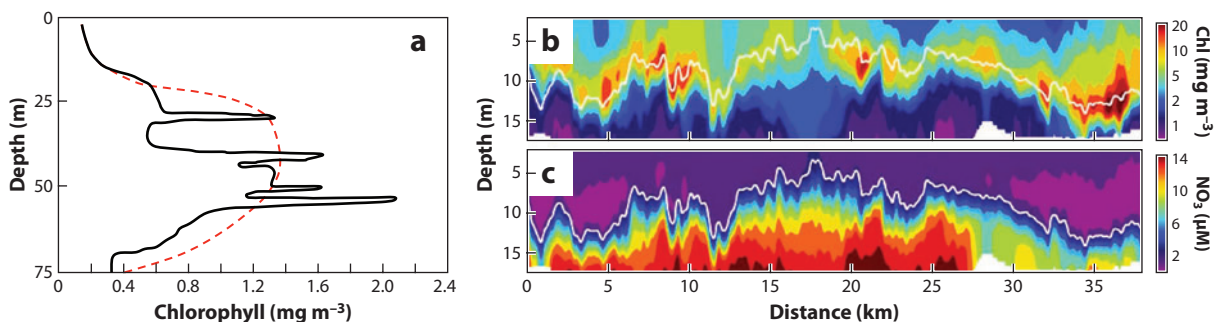
Figure 1

Technological advances over the past four decades have greatly improved our ability to characterize the spatial distribution of phytoplankton. (*a*) Thin layers observed in 1967 off La Jolla, California. The black line shows the continuous vertical chlorophyll concentration profile measured using a submersible pump and a ship-based fluorometer. The red dashed line shows the profile obtained using values from discrete depths, mimicking what would be obtained from bottle casts. This study revealed that the vertical distribution of phytoplankton often contains fine-scale spatial variability that eluded quantification by traditional sampling techniques. (*b*) Thin layers of chlorophyll (Chl), likely dominated by the flagellate *Akashiwo sanguinea*, observed at night in Monterey Bay using an autonomous underwater vehicle. (*c*) Concurrent measurements revealing that the upper portion of the water column was depleted of nitrate. Layers formed at night, as a result of downward vertical migration to the nutricline. Phytoplankton cells aggregated at the 3-μM nitrate isocline (*white line* in panels *b* and *c*). Panel *a* adapted with permission from Strickland (1968), copyright © 1968 by the American Society of Limnology and Oceanography Inc.; panels *b* and *c* adapted with permission from Ryan et al. (2010), copyright © 2010 by Elsevier B.V.

depth. Indeed, traditional techniques for the enumeration of plankton, including nets and bottles, lack the spatial resolution to capture the strong, sharp peaks in cell concentration characteristic of thin layers, resulting in the thinnest phytoplankton peaks being smeared or missed altogether (Donaghay et al. 1992).

In the past 15 years we have seen a renaissance of thin layer observations, triggered by major advances in our ability to quantify thin layers of phytoplankton—and zooplankton, which prey on them—in situ. Examples include new techniques in optical sensing (Cowles et al. 1998, Twardowski et al. 1999), acoustic sensing (Benoit-Bird et al. 2009, 2010; Holliday et al. 1998), underwater imaging (Alldredge et al. 2002, Prairie et al. 2010), and airplane-based LIDAR (light detection and ranging; Churnside & Donaghay 2009). Observations of thin layers have now been made in many locations around the world, mostly in the coastal ocean but also in the open ocean (Churnside & Donaghay 2009, Hodges & Frantantoni 2009). Simultaneously, a number of mechanisms have been put forward to explain the convergence of phytoplankton into thin layers.

Here we review key findings from thin layer observations, describe proposed mechanisms of convergence and the methods used to decipher them in field observations, and discuss the ecological interactions of phytoplankton layers with higher trophic levels. We argue that the time is ripe for the next phase of thin layer research, focusing on the development of a quantitative, predictive framework for the processes that shape layer formation and on the formulation of new field and laboratory approaches to better understand their ecological repercussions.

2. CHARACTERISTICS OF THIN PHYTOPLANKTON LAYERS

2.1. How Are Thin Layers Different from Other Phytoplankton Aggregations?

Heterogeneity in the distribution of phytoplankton encompasses a wide range of spatial and temporal scales. How then are thin phytoplankton layers different from other phytoplankton aggregations? Thin layers are readily distinguished from deep chlorophyll maxima by their vertical extent: Deep chlorophyll maxima are typically tens of meters thick, with relatively weak vertical gradients in phytoplankton concentration (Cullen 1982), whereas thin layers have thicknesses of a fraction of a meter to a few meters, much stronger vertical concentration gradients (Dekshenieks et al. 2001), and can harbor phytoplankton concentrations much greater than the background (Section 2.5).

At the other end of the spectrum, thin layers differ from ephemeral centimeter-scale patches (Gallager et al. 2004, Mitchell et al. 2008, Waters et al. 2003) in both shape and persistence time. Thin layers are pancake shaped, have aspect ratios (horizontal to vertical extent) often in excess of 1,000 (Moline et al. 2010) and last hours to weeks (see Section 2.6), whereas small-scale patches have an aspect ratio closer to unity and lifetimes of minutes (Mitchell et al. 2008).

2.2. Criteria for the Identification of Thin Layers

The use of universal criteria to define which phytoplankton aggregations constitute thin layers can facilitate consistent comparisons among observations made at different times and locations by different researchers. A number of independent criteria have been developed, most of which share three requirements (Dekshenieks et al. 2001, Sullivan et al. 2010b): (*a*) The aggregation must be spatially and temporally persistent (e.g., readily identifiable in two subsequent vertical profiles), (*b*) the vertical extent of the aggregation must not exceed a threshold (e.g., 5 m), and (*c*) the maximum concentration must exceed a threshold (e.g., three times the background). Thresholds differ among studies, and some studies use additional criteria. Experience has revealed that a single

criterion cannot be applied to all thin layers, given the diversity of organisms, instrumentation, and environmental conditions (Sullivan et al. 2010b). However, when possible, there is significant value in using consistent criteria to identify layers.

2.3. Horizontal Extent of Thin Layers

Thin layers have traditionally been observed with vertical profiles of the water column, and information on their horizontal extent is thus often in short supply (for an overview of studies that measure horizontal layer dimensions, see Cheriton et al. 2010). Moline et al. (2010) performed an extensive analysis of the spatial decorrelation scale of chlorophyll in Monterey Bay using data collected with two autonomous underwater vehicles and a ship-based system. The horizontal scale decreased dramatically over the course of a few years: In 2002 and 2003, the average layer length was ≈7 km, whereas in 2006 and 2008, it was just ≈1 km. This decrease was correlated with a shift in Monterey Bay's taxonomic composition, from nonmotile diatoms[1] to motile dinoflagellates, during the summer of 2004 (Jester et al. 2009, Rines et al. 2010). The relation between motility and horizontal layer extent remains largely unexplored.

Layers can be considerably larger in some environments. For example, Hodges & Fratantoni (2009) observed a thin layer off the continental shelf in the Philippine Sea that was >75 km long, while Nielsen et al. (1990) reported on a persistent, largely monospecific thin layer in the Kattegat/Skagerrak (the strait connecting the North and Baltic Seas) that extended for hundreds of kilometers.

2.4. Frequency of Occurrence of Thin Layers

The frequency of occurrence of thin layers varies greatly with geographical location and time of day. Dekshenieks et al. (2001) found thin layers in 54% of 120 profiles collected during three multiday cruises in East Sound, Washington, and Steinbuck et al. (2010) found them in 21% of 456 profiles collected over two weeks in the Gulf of Aqaba (Red Sea). Benoit-Bird et al. (2009) observed strong diel variation: out of 632 profiles collected over a three-week period in Monterey Bay, thin layers were found in only 2% of the profiles acquired during the daytime but in 29% of those collected at night.

Using 80,000 km of airplane-based LIDAR measurements, Churnside & Donaghay (2009) found thin layers to be relatively common in some regions. Off the Oregon and Washington coasts, they occurred 19% (during the daytime) and 6% (at night) of the time over a 9-day period. In contrast, near Kodiak Island, Alaska, thin layers were found only 1.6% (during the daytime) and 0.2% (at night) of the time over a three-week period. These results come with some caveats, as LIDAR does not detect layers beyond a certain depth (≈20 m) and, more importantly, cannot discriminate among phytoplankton, zooplankton, and other particles (Churnside & Donaghay 2009).

The variability in the frequency of occurrence can be large even in a single location. For example, analysis of data from Monterey Bay revealed thin phytoplankton layers 87%, 56%, and 21% of the time over 1–3-week sampling periods in 2002, 2005, and 2006, respectively (Sullivan et al. 2010a). As suggested above, these changes might have been driven by a shift in the community composition.

---

[1]Although some diatoms can glide along surfaces, they are largely incapable of motility in the water column and will thus be considered nonmotile for the purposes of this review.

2.5. Concentration Enhancement and Depth-Integrated Phytoplankton Fraction

Two metrics are often used to quantify the intensity of a thin layer: (*a*) the maximum phytoplankton concentration within the layer, relative to the background, and (*b*) the fraction of phytoplankton contained within the layer, relative to the total amount in the water column. In terms of the first metric, peak phytoplankton concentrations within a thin layer can be nearly two orders of magnitude larger than the background. For example, Ryan et al. (2008) reported a maximum chlorophyll concentration that was 55 times above the background. More typically, peak concentrations are several times that of the background (McManus et al. 2003, Sullivan et al. 2010a). This metric is directly relevant to processes that rely on encounter rates, such as the formation and subsequent settling of aggregates, sexual reproduction, and cell-cell communication, all of which to the first order scale with the square of cell concentration. In terms of the second metric, observations have revealed that a substantial fraction of the phytoplankton in the water column can reside within a thin layer. For example, Sullivan et al. (2010a) found that, based on chlorophyll concentrations, this fraction ranged from 33% to 47% in Monterey Bay.

2.6. Persistence Time of Thin Layers

Thin layers persist for periods ranging from hours to weeks. Layers detected at night in the nutricline in Monterey Bay lasted only a few hours (Sullivan et al. 2010a), whereas pycnocline-associated layers in East Sound lasted for days (Menden-Deuer & Fredrickson 2010) and layers in the Kattegat/Skagerrak persisted for weeks (Bjornsen & Nielsen 1991, Nielsen et al. 1990). However, tracking a thin layer from its formation to its demise is challenging because of the extensive sampling effort required and the advection of the layer by the ambient flow. Thus, layer persistence time remains difficult to measure, hindering quantitative comparisons with mathematical predictions (see Section 3).

2.7. Correlation with Stratification and Shear

The depths at which thin layers occur are frequently correlated with strong gradients in fluid density (stratification) and vertical shear, both of which tend to occur at the bottom of the mixed layer (Johnston & Rudnick 2009).

Stratification plays a dual role in layer formation. First, it can produce layers because sinking cells often reach neutral buoyancy at a pycnocline, where they accumulate (see Section 3.3). Second, stratification stifles vertical turbulent dispersion, favoring layer formation by other mechanisms (see Section 3). The importance of stratification is supported by the observation that thin layers are often correlated with thermoclines (Steinbuck et al. 2009) or haloclines (Rines et al. 2002). For instance, Dekshenieks et al. (2001) found that 71% of the thin layers they observed in East Sound in 1996 were associated with a pycnocline.

Layers often occur where the horizontal velocity sharply changes direction over depth, and some mechanisms invoke shear as a means of layer formation (see Sections 3.1 and 3.4). Ryan et al. (2008) found that 92% of the thin layers they recorded in Monterey Bay in 2003 were associated with peaks in shear, with a mean shear rate of $S \approx 0.02 \text{ s}^{-1}$. Dekshenieks et al. (2001) reported that thin layers in East Sound were thinnest during spring tides, when shear was enhanced within layers ($S = 0.003$–0.09 s^{-1} for all layers). Cheriton et al. (2009) found that the shear rate within a thin layer in Monterey Bay oscillated about a mean value of $S \approx 0.07 \text{ s}^{-1}$ over an 8.5-h period, at times exceeding 0.1 s^{-1}. Layers can occur at different positions relative to the peak in shear: Ryan et al.

Nutricline: region of the water column characterized by strong vertical gradients in nutrient concentration, with typical concentrations increasing with depth

Pycnocline: region of the water column characterized by strong vertical gradients in fluid density due to salinity gradients (halocline), temperature gradients (thermocline), or both

Hydrodynamic shear (or shear): a change in fluid velocity over distance; here we consider vertical shear, $S = \mathrm{d}u/\mathrm{d}z$, the change in the horizontal velocity, u, over depth, z

Turbulent dispersion: the spreading of a scalar (e.g., a solute or a plankton population) resulting from stirring and mixing by turbulent fluid motion

(2008) found the maximum shear in the middle of layers, whereas Sullivan et al. (2010a) observed shear to peak 1–2 m above the layers. A note of caution is in order when interpreting shear rates, because in several cases these are obtained with acoustic Doppler current profilers, which can systematically underestimate shear maxima owing to coarse (meter-scale) sampling resolutions (Cowles 2004).

Shear is a double-edged sword for thin layers: it can favor layer formation via straining (see Section 3.1) or gyrotactic trapping (see Section 3.4), but it can also trigger hydrodynamic instabilities and turbulence that dissipate layers. These instabilities are resisted by stratification, and the net stability of the water column is determined by the gradient Richardson number, $Ri = N^2/S^2$, which measures the relative importance of stratification and shear: When $Ri < 1/4$, the water column is expected to be unstable (Kundu & Cohen 2004). This prediction is corroborated by observations in East Sound that found no layers when $Ri < 0.23$ (Dekshenieks et al. 2001), likely because of dissipation due to turbulence.

2.8. Phytoplankton Motility

Approximately 90% of the phytoplankton species known to form harmful algal blooms (HABs) can actively swim (Smayda 1997). Vertical migration allows cells to shuttle to depth at night, where limiting nutrients are abundant and predation risks reduced (Bollens et al. 2011), and to reside in the well-lit surface waters during the day (Ryan et al. 2010, Sullivan et al. 2010a). Many thin layers are composed of motile cells (Bjornsen & Nielsen 1991, Koukaras & Nikolaidis 2004, Nielsen et al. 1990, Steinbuck et al. 2009, Sullivan et al. 2010a, Townsend et al. 2005, Tyler & Seliger 1978), although thin layers of nonmotile species, such as diatoms, are also frequent (Alldredge et al. 2002, Stacey et al. 2007, Sullivan et al. 2010a). However, a comprehensive knowledge of the role that motility plays in layer formation is still lacking, partly because the species composition of many layers remains undetermined.

The overwhelming majority of motile phytoplankton species are eukaryotic and swim by propagating bending waves along their flexible flagella (Guasto et al. 2012). The arrangement and kinematics of the flagella are diverse: Some green algae beat two nearly identical flagella in a breaststroke motion (Polin et al. 2009), whereas most dinoflagellates wave two dissimilar flagella in combination for propulsion and steering (Fenchel 2001). For some species, the mechanism of propulsion remains unknown, as in *Synechococcus*, which lacks flagella (Brahamsha 1999, McCarren & Brahamsha 2009). Swimming velocities of phytoplankton vary widely: The motile clade of *Synechococcus* ($\approx$1-μm diameter) swims at up to $w_s \approx 25$ μm s^{-1} (Waterbury et al. 1985), whereas larger eukaryotic cells (tens of micrometers in diameter) can swim at $w_s = 100$–500 μm s^{-1} (Fauchot et al. 2005, Kamykowski et al. 1992, Sullivan et al. 2010a). Care should be taken when interpreting swimming velocities, as they are often measured along the cell trajectory. The net migration speed (e.g., the vertical projection of the swimming velocity) can be considerably lower because of randomness in the swimming direction (Hill & Häder 1997) or the influence of turbulent shear (Durham et al. 2011).

2.9. Thin Layers of Toxic Species

Thin layers are often trophic hotspots, correlated with high abundance of bacteria, zooplankton, and fish (Benoit-Bird et al. 2009, 2010; McManus et al. 2003, 2008) (see Section 5). In contrast, some thin layers composed of toxic phytoplankton exhibit lower zooplankton concentrations than the surrounding waters (Bjornsen & Nielsen 1991, Nielsen et al. 1990), suggesting that aggregation into layers provides a selective advantage by offering a refuge from predation. Many toxic species

have been observed to form thin layers, including *Pseudo-nitzschia australis* (McManus et al. 2008), *Chrysochromulina polylepis* (Nielsen et al. 1990), *Gyrodinium aureolum* (Bjornsen & Nielsen 1991), *Dinophysis* spp. (Koukaras & Nikolaidis 2004), *Alexandrium fundyense* (Townsend et al. 2005), and *Prorocentrum minimum* (Tyler & Seliger 1978).

Whereas some zooplankters suffer deleterious effects, including death, from toxic phytoplankton and avoid aggregations of toxic species, others predate on them seemingly with impunity (Nielsen et al. 1990, Turner & Tester 1997). These immune zooplankters might substantially increase their foraging rate within a thin layer, compared to when they are exposed to a homogeneous prey distribution, and thereby enhance the transfer of toxins up the marine food web. Thus, toxic species might pose a greater risk to higher trophic levels, such as marine mammals and seabirds, when they are concentrated in a thin layer (McManus et al. 2008).

Toxic thin layers are believed to play an important role in the instigation of HABs (Donaghay & Osborn 1997, Gentien et al. 2005, McManus et al. 2008, Sellner et al. 2003). Because large quantities of cells can be harbored meters beneath the surface, thin layers pose a challenge for the detection of subsurface blooms that might later spread to the entire water column. Monitoring programs relying on surface sampling or coarse sampling over depth might miss a thin layer, offering little warning time, for example, to alert fishery managers (McManus et al. 2008). Although many factors contribute to HABs (Smayda 1997), accounting for thin layer dynamics in existing HAB models (after Franks 1997) may hold the key to improving our ability to both understand and predict these events (Donaghay & Osborn 1997).

Tyler & Seliger (1978) found that in Chesapeake Bay, thin layers play a crucial role in annual blooms of the toxic dinoflagellate *P. minimum*, a species responsible for shellfish poisoning in humans (Heil et al. 2005). Every year, a population of *P. minimum* near the bay's mouth forms a thin layer, which is transported by density currents over 200 km upstream into shallower waters. During the journey the layers receive little light at depth, which limits growth. As layers reach shallower depths and light becomes abundant, a large bloom occurs. This surface bloom is eventually transported back to the mouth of the bay, forming the basis of the following year's bloom. Sellner et al. (2003) conjectured that a similar seeding process is responsible for *Dinophysis* blooms along the coasts of Spain and Sweden and for *Karenia mikimotoi* blooms in the English Channel.

Toxic thin layers do not have to instigate a surface bloom to profoundly affect the marine ecosystem. Perhaps the most striking example of the destructive potential of a thin layer is the pycnocline-associated layer of the toxic flagellate *C. polylepis* that formed in 1988 over 75,000 km^2 of the Skagerrak and Kattegat, which killed ≈10 million euros worth of farmed fish and ravaged the natural pelagic and benthic communities (Gjosaeter et al. 2000). The mortality of some pelagic organisms, such as codfish, was very high during the bloom, but the most dramatic repercussions of the thin layer occurred in the benthos, demonstrating the complex feedbacks in the marine ecosystem. Heavy mortality of sea stars and other predators greatly favored the mussel *Mytilus edulis*, which remained largely unaffected by the *Chrysochromulina* toxin and thus outcompeted other sessile organisms (cf. Paine 1966). Significantly increased numbers of mussel beds persisted for 2 years, until their predators rebounded and the sublittoral zone recovered. (Gjosaeter et al. 2000).

3. MECHANISMS OF LAYER FORMATION AND PERSISTENCE

Several mechanisms have been proposed to explain the formation and persistence of thin layers. Here we present and contrast these mechanisms as a basis for interpreting observations of thin layers in the field.

3.1. Straining of Phytoplankton Patches by Shear

Vertical gradients in horizontal velocity can transform horizontal gradients of scalars into vertical gradients. This occurs by differential advection, whereby portions of a patch at different depths are transported at different flow velocities, until the patch is transformed into a thin layer (**Figures 2a** and **3a,b**). This mechanism, proposed by Eckardt (1948) to explain field observations of fine-scale vertical variability in temperature, was later extended to thin phytoplankton layers (Franks 1995, Osborn 1998). Here we summarize the spatial and temporal scales that characterize
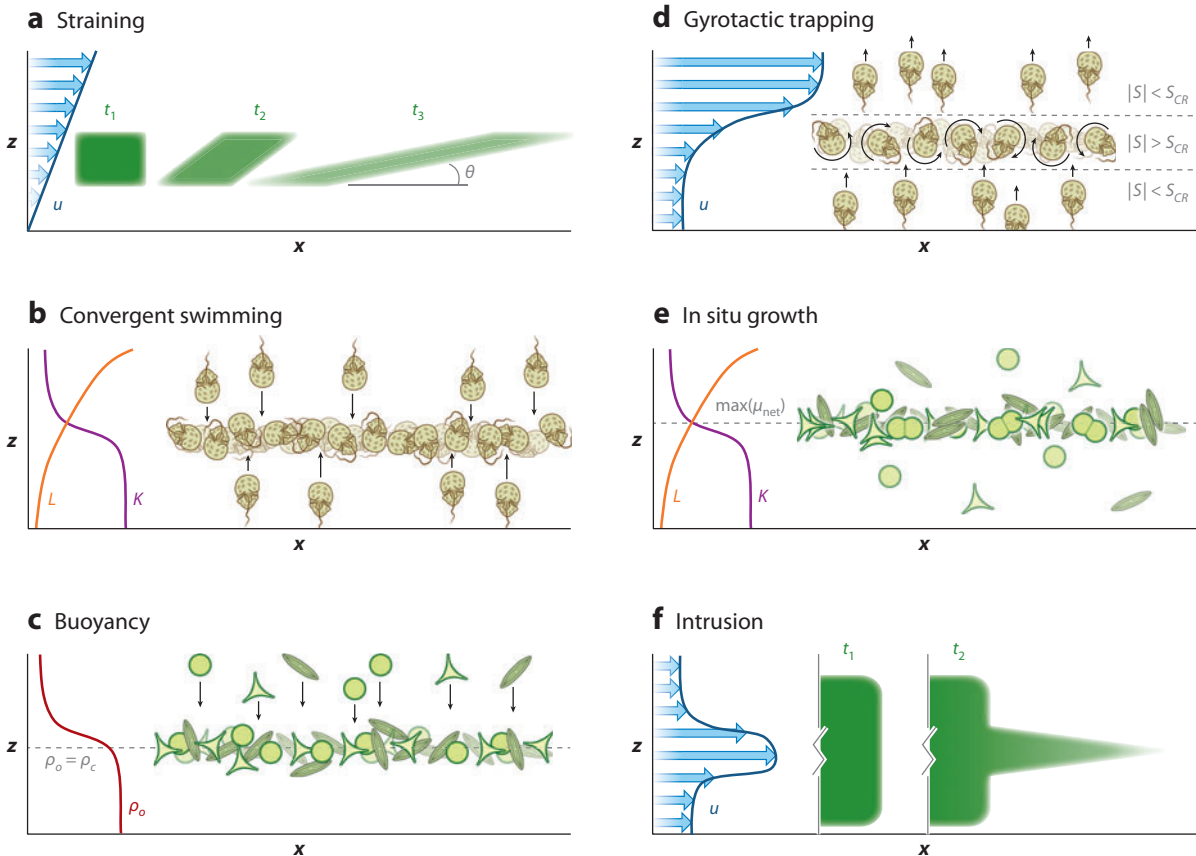

Figure 2

Diverse mechanisms can drive the formation of thin phytoplankton layers. (*a*) Straining transforms initial (time t_1) horizontal phytoplankton heterogeneity into a thin layer (t_3), by progressively tilting (t_2) a phytoplankton patch. This effect results from the differential advection of the patch over depth (see Section 3.1). The change in color from t_1 to t_3 (*less green*) indicates a lower concentration of phytoplankton. (*b*) The accumulation of cells in layers can also result from directed motility, guided by cues that drive cells towards desirable conditions (e.g., a specific light intensity, *L*, or nutrient concentration, *K*; see Section 3.2). (*c*) Nonmotile cells whose density differs from that of the surrounding water sink (if heavier) or rise (if lighter) and accumulate at their depth of neutral buoyancy (*dotted line*), typically occurring at pycnoclines (see Section 3.3). (*d*) The vertical migration of motile phytoplankton can be suppressed in regions of high fluid shear, forming layers through gyrotactic trapping. As cells swim into a region where the magnitude of the shear rate, |*S*|, exceeds a threshold, S_{CR}, flow induces tumbling of the cells, trapping them at depth in the form of a thin layer (see Section 3.4). (*e*) Thin layers can also form when growth rates are enhanced at mid-depth. For example, this can occur when light intensity and nutrient concentration are both suitable for growth over a small depth interval (as shown here). The depth of maximal growth rate is denoted by a dotted line (see Section 3.5). (*f*) Intrusions can form thin layers by transporting waters containing high phytoplankton concentrations into adjacent waters containing lower concentrations (see Section 3.6).

layer formation by straining, following the scaling analysis by Stacey et al. (2007) and the comprehensive treatment of Birch et al. (2008), who considered the straining of a two-dimensional Gaussian patch.

A phytoplankton patch in a vertically sheared flow will lengthen and, after a transient, become thinner (**Figures 2a** and **3a**). For simplicity, we consider that the shear rate du/dz—where $u(z)$ is the horizontal fluid velocity—is constant in time and uniform over depth and denote it by S_u. Then the horizontal extent of a patch with initial length L_o and thickness H_o grows like $L(t) \sim [L_o^2 + (H_o S_u t)^2]^{1/2}$. After a time $t_{shear} \sim L_o/(S_u H_o)$, the upper portion of the patch has been transported horizontally past the lower portion. Up to this time, the layer thickness H_o remains unchanged, whereas for $t > t_{shear}$, the layer thickness measured across the mid-section of the strained patch decreases as $H(t) \sim L_o/(S_u t)$ (Birch et al. 2008, Stacey et al. 2007).

Typical values of vertical shear rates in the ocean are on the order of $S \sim 0.01$ s^{-1} (MacKinnon & Gregg 2003), although values of $S \sim 0.1$ s^{-1} have been measured within thin layers (Cheriton et al. 2009, Dekshenieks et al. 2001), and larger shear rates might be revealed by sampling at higher vertical resolution (Cowles 2004). The size of phytoplankton patches before straining is highly variable, and we consider here a patch of initial size $H_o = 10$ m and $L_o = 1$ km as an example. When strained, a patch of these dimensions will begin decreasing in thickness after $t_{shear} \sim 3$ h for $S_u = 0.01$ s^{-1}. A distinctive characteristic of patches created by straining is their tilt across surfaces of constant density. Although small, this tilt has allowed the identification of patch straining as the mechanism responsible for the formation of some observed layers (Hodges & Fratantoni 2009, Prairie et al. 2010).

In the absence of turbulent dispersion, the thickness of a layer strained by fluid shear would monotonically approach zero, and the phytoplankton concentration in the layer would remain unchanged (unlike the other mechanisms described in this section, straining cannot increase the local concentration of phytoplankton). However, turbulence acts to dissipate the layer, reducing peaks in phytoplankton concentration and increasing the layer thickness, thus placing a limitation on the lifetime and intensity of strained layers. Layers can form by way of this mechanism only if a patch is strained into a layer before turbulent dispersion mixes it away. In other words, dispersion must be weak compared to patch straining. In the ocean, turbulent dispersion is much larger in the horizontal (x) than in the vertical (z) direction, with typical eddy diffusivities on the order of $\kappa_x = 1$ m^2 s^{-1} and $\kappa_z = 10^{-5}$ m^2 s^{-1}. The relative importance of straining and turbulent dispersion is quantified by the horizontal and vertical Péclet numbers, $Pe_x = S_u H_o L_o/\kappa_x$ and $Pe_z = S_u H_o^3/L_o \kappa_z$, defined as the ratio of the timescales for horizontal and vertical dispersion, L_o^2/κ_x and H_o^2/κ_z, respectively, to the straining timescale t_{shear}. For a thin layer to form before dissipating, it is necessary that $Pe_x \gg 1$ and $Pe_z \gg 1$ (Birch et al. 2008). For example, if $S_u = 0.01$ s^{-1}, $\kappa_x = 1$ m^2 s^{-1}, $\kappa_z = 10^{-5}$ m^2 s^{-1}, $H_o = 10$ m, and $L_o = 1$ km, then $Pe_x = 100$ and $Pe_z = 1,000$; hence conditions are conducive to layer formation by straining.

After a time $t = t_{shear}$, the layer begins thinning. The rate of thinning decreases with time (**Figure 3a**), until it equals the rate of layer thickening by vertical dispersion. The minimum thickness, $H_{min} \sim (\kappa_z L_o/S_u)^{1/3}$, is reached when vertical dispersion and straining balance, which occurs at time $t_{min} \sim (L_o^2/\alpha^2 \kappa_z)^{1/3}$ (Birch et al. 2008, Stacey et al. 2007). At this time the layer's angle of tilt (**Figure 2a**) is $\theta \sim (\kappa_z/S_u L_o^2)^{1/3}$ (Stacey et al. 2007). For $t < t_{min}$, the layer thickness decreases as straining dominates over dispersion, whereas the opposite is true for $t > t_{min}$. For the values above, the patch reaches a minimum thickness of $H_{min} \sim 1$ m after $t_{min} \sim 1$ day.

Because straining does not actively concentrate cells, turbulent dispersion acts to monotonically reduce peak concentrations in the layer. For typical parameter ranges, the layer intensity—defined as the current maximum in cell concentration normalized by the maximum initial concentration—declines like $I(t) \sim [1 + 2(t/t_{min})^3]^{-1/2}$ (Birch et al. 2008). At $t = t_{min}$, the layer's

Eddy diffusivity:
a parameter with the dimensions of a diffusion coefficient (length^2/time) that quantifies how rapidly a scalar is dispersed by turbulent fluid motion
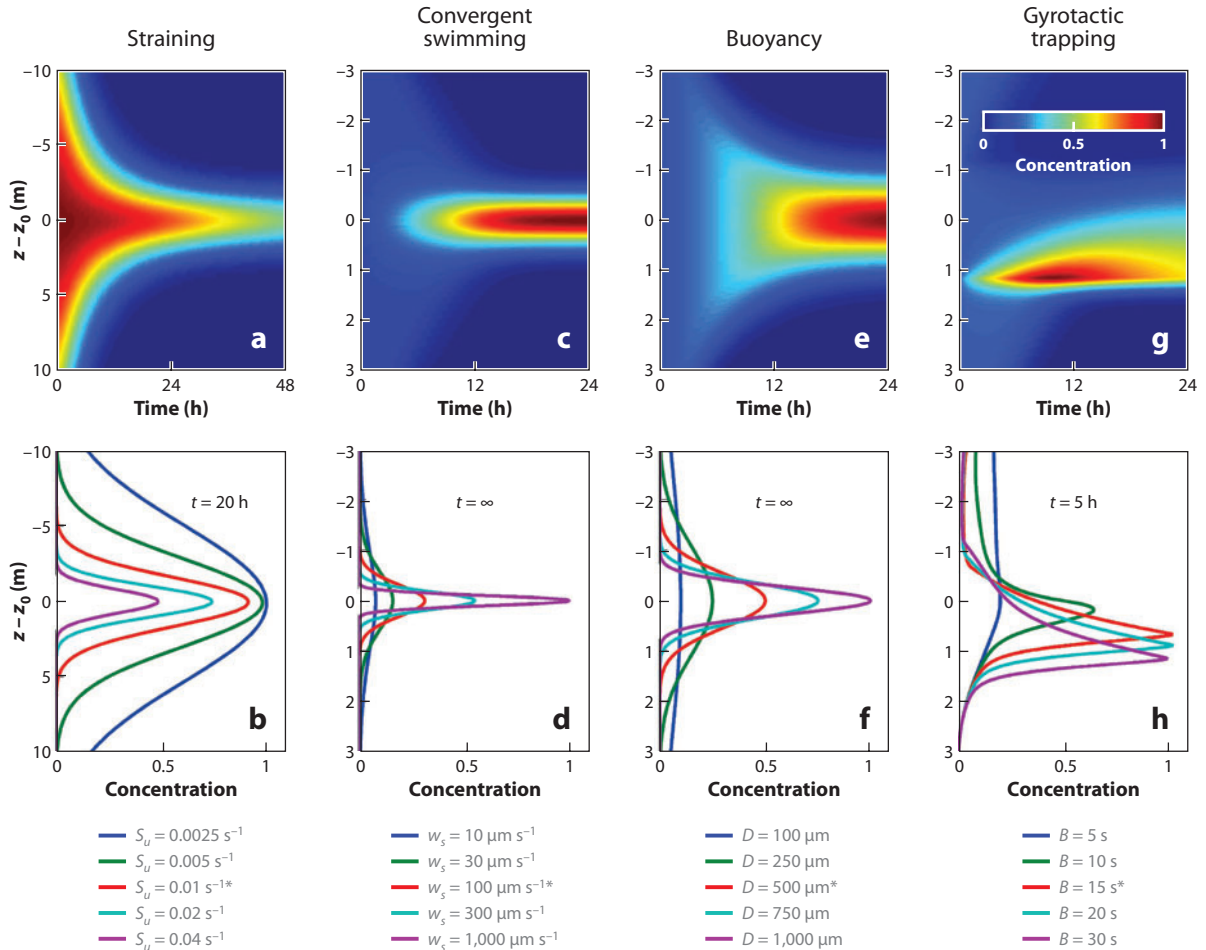
Péclet number:
here, dimensionless parameter that determines the relative importance of transport by advection or motility to transport by turbulent dispersion

maximum concentration is still ∼60% of its initial concentration. After t_{min}, the concentration falls off rapidly: At $t = 4t_{min}$ (∼4 days in the above example), it is only ∼10% of the initial concentration. Eventually, vertical dispersion returns the layer thickness to its initial value, H_o, after a time H_o^2/κ_z. By this time, however, the layer intensity is only marginally above background and of little ecological relevance (Birch et al. 2008).

3.2. Convergent Swimming

Many factors can contribute to the aggregation of cells at a particular depth by convergent swimming. There is evidence that gradients in nutrient concentration often act in concert with light cues. In laboratory experiments, MacIntyre et al. (1997) found that the HAB-forming dinoflagellate *Alexandrium tamarense* did not perform any vertical migration under uniformly nitrate-replete conditions. When nitrate was exhausted in the upper portion of the water column, the population initiated a diel migration to the nutricline. The migration began just before dark, and phytoplankton swam back to the surface before sunrise, indicating that the migration was not driven purely by phototaxis. Field observations have confirmed this behavior: For example, *Akashiwo sanguinea* has been reported to initiate downward migration to the nutricline 5–6 h before sunset and to begin

Straining	Convergent swimming	Buoyancy	Gyrotactic trapping
$S_u = 0.0025$ s^{-1}	$w_s = 10$ μm s^{-1}	$D = 100$ μm	$B = 5$ s
$S_u = 0.005$ s^{-1}	$w_s = 30$ μm s^{-1}	$D = 250$ μm	$B = 10$ s
$S_u = 0.01$ s^{-1}*	$w_s = 100$ μm s^{-1}*	$D = 500$ μm*	$B = 15$ s*
$S_u = 0.02$ s^{-1}	$w_s = 300$ μm s^{-1}	$D = 750$ μm	$B = 20$ s
$S_u = 0.04$ s^{-1}	$w_s = 1{,}000$ μm s^{-1}	$D = 1{,}000$ μm	$B = 30$ s

its upward journey 3–4 h before sunrise (Sullivan et al. 2010a). The onset of vertical migration before light becomes a cue is common to many species (e.g., Baek et al. 2009) and is likely driven by cell metabolism (Kamykowski & Yamazaki 1997). Furthermore, concentrated cells within thin layers might themselves affect light penetration, changing the light cues available to cells (Marcos et al. 2011, Sullivan et al. 2010a).

Some thin layers occur at depths corresponding to specific nutrient concentrations. Ryan et al. (2010) observed that *A. sanguinea* aggregated within a vertical gradient of nitrate in Monterey Bay. Chlorophyll peaks coincided with the depth of the 3-μM nitrate isocline, demonstrating that cells swam downward until they reached this concentration (**Figure 1b,c**). The half-saturation constant for nitrate uptake by this species is 1 μM (Kudela et al. 2010), suggesting that swimming deeper to higher nitrate concentrations might not have been justified by the small additional uptake. In the Gulf of Maine, Townsend et al. (2005) found that a thin layer of *A. fundyense* resided at a depth corresponding to a cumulative concentration of nitrate plus nitrite of 1 μM, while another fraction of the population was located near the surface. This bimodal distribution might have resulted from asynchronous vertical migrations within the population (Ralston et al. 2007). This explanation assumes that when all steps of the migration cycle (i.e., photosynthesizing near the surface, swimming to depth, absorbing nutrients, and swimming back to the surface) cannot be completed in 24 hours, the cells' migration pattern becomes desynchronized from the day/night cycle, leading to two peaks in cell abundance, one at the surface and one at depth, between which individuals shuttle (Ralston et al. 2007).

Gradients in salinity (haloclines) also attract motile phytoplankton. The toxic raphido-phyte *Heterosigma akashiwo*, sometimes observed in thin layers (Grünbaum 2009), has been shown to aggregate at haloclines in laboratory water columns (Harvey & Menden-Deuer 2011). Natural phytoplankton assemblages also aggregate at haloclines in the laboratory, indicating that convergent swimming to salinity gradients might be widespread, although the fitness benefit of this behavior remains unknown (D. Grünbaum, personal communication).

←———

Figure 3

Thin layers generated via different convergence mechanisms exhibit distinctive characteristics. Using the mathematical models described in Section 3, we illustrate typical layer morphologies produced by four different convergence mechanisms. (*Lower panels*) Vertical profiles of phytoplankton concentration, $c(z)$, at a specific time t (or at steady state, denoted by $t = \infty$) for five different parameter values (indicated below each panel). (*Upper panels*) The spatiotemporal development of the layer for the value of the parameter marked with an asterisk. The color bar denotes cell concentration. All plots assume a vertical eddy diffusivity $\kappa_z = 10^{-5}$ m^2 s^{-1}, and concentrations have been rescaled to a maximum of $c = 1$ in each case (taking advantage of the linearity of the advection-diffusion equation). (*a,b*) Layer formation via straining occurs when horizontal heterogeneity in a phytoplankton distribution is transformed into vertical heterogeneity. Straining cannot elevate phytoplankton concentrations above the maximum initial concentration. We assumed a Gaussian initial distribution centered at the origin, with standard deviations $L_o = 1$ km and $H_o = 10$ m; $u(z = 0) = 0$; a homogenous shear rate S_u; and $\kappa_x = 1$ m^2 s^{-1} (see Section 3.1). Shown are concentrations at $x = 0$, where they are highest. (*c,d*) Convergent swimming ($\delta = 1$ m, $z_o = 0$, and $P = 1$; see Section 3.2) assumes that cells above the layer swim downward and cells below the layer swim upward, yielding a steady balance between motility and turbulent dispersion. Faster swimming speeds w_s produce thinner layers. (*e,f*) Cell buoyancy ($N = 0.05$ s^{-1}, $\nu = 10^{-6}$ m^2 s^{-1}, $z_o = 0$, and $P = 1$; see Section 3.3) produces thin layers in a manner analogous to convergent swimming, albeit for nonmotile cells: Cells above their neutral buoyancy depth z_o sink, whereas those below it rise. A steady state is reached when buoyant convergence balances turbulent dispersion. Larger cells form thinner layers because the buoyancy velocity increases with size. (*g,h*) Gyrotactic trapping produces asymmetric layers (because swimming direction is asymmetric; here, upward) that do not attain a steady state because cells escape through one side (here, the top) of the layer by turbulent dispersion, which releases them from the trapped region. For the parameters used here ($\delta = 1$ m, $z_o = 0$, $u_o = 0.1$ m s^{-1}, and $w_{max} = 100$ μm s^{-1}; see Section 3.4) the maximum shear rate is $S = u_o/\delta = 0.1$ s^{-1}; therefore, layer formation occurs only for $B \gtrsim 10$ s. Results in panels *c*, *d*, *g*, and *h* were produced via numerical integration, assuming an initially homogeneous concentration field ($c = 1$ for all z). Panels *d* and *f* show analytical expressions (Equations 2 and 3). Results in panels *a* and *b* were obtained via numerical integration of the two-dimensional advection-diffusion equation.

Thin layer formation induced by an active swimming response (e.g., toward a preferred nutrient, salinity, or light level) is often modeled by assuming that cell motility is directed to a particular depth (**Figure 2b**). Stacey et al. (2007) proposed a simple model of convergent swimming, in which cells swim vertically toward a target depth z_o from both above and below that depth, at a constant speed w_s. If we denote by $W(z)$ the vertical swimming speed at depth z (with z and W positive downward), the behavior modeled by Stacey et al. (2007) corresponds to $W(z) = -w_s$ for $z > z_o$ and $W(z) = w_s$ for $z < z_o$. However, gradients in stimuli (e.g., nutrients, salinity, light) and the timescale over which cells respond to these stimuli are likely not as abrupt as this minimum-ingredient model assumes (Ryan et al. 2010, Sullivan et al. 2010a). An additional degree of realism can be included in the model by assuming a reduction in the swimming speed as the target depth z_o is approached, to avoid a discontinuous change in swimming behavior at z_o. This was proposed by Birch et al. (2009), who considered the continuous velocity $W(z) = -w_s \tanh[(z - z_o)/\delta]$. In this formulation, cells swim toward the target depth z_o with a vertical velocity whose magnitude smoothly increases with distance from z_o, reaching a maximum speed of w_s at a vertical distance of order δ from the target depth. At the target depth, the swimming speed is zero; $W(z = z_o) = 0$. Although more realistic than the binary behavioral model of Stacey et al. (2007), this model requires the estimation of the length scale δ. The two models are equivalent in the limit $\delta \to 0$.

Unlike patch straining (see Section 3.1), thin layer formation via convergent swimming is inherently a one-dimensional process. The spatiotemporal evolution of the cell concentration, $c(z,t)$, can thus be predicted by the one-dimensional advection-diffusion equation

$$\frac{\partial c}{\partial t} + \frac{\partial (c\,W)}{\partial z} = \frac{\partial}{\partial z}\left(\kappa_z \frac{\partial c}{\partial z}\right), \tag{1}$$

where the second term on the left-hand side is the divergence of the cell flux that results from vertical swimming. Unlike straining, the vertical distribution of cells in a thin layer that forms by convergent swimming can reach a steady state, in which the flux of cells into the thin layer due to swimming balances the flux of cells out of the layer due to turbulent dispersion. Using Stacey et al.'s (2007) assumption of binary convergent swimming leads to the prediction that the steady-state layer thickness scales as $H_e \sim \kappa_z/w_s$. Convergent swimming can therefore produce layers that are very thin: Cells swimming at $w_s = 100$ μm s^{-1} in an environment with vertical eddy diffusivity $\kappa_z = 10^{-5}$ m^2 s^{-1} accumulate in a layer that is only $H_e \sim 10$ cm thick.

A reduction in swimming speed as cells approach the target depth z_o can increase layer thickness. Using their continuous swimming velocity profile, Birch et al. (2009) obtained the steady-state cell distribution

$$c_e(z) = \frac{P}{\delta} \frac{\cosh[(z - z_o)/\delta]^{-Pe_{swim}}}{\beta(\frac{1}{2}, \frac{1}{2}Pe_{swim})}, \tag{2}$$

where P is the depth-integrated phytoplankton concentration (cells per unit surface area of the ocean), and $Pe_{swim} = w_s\delta/\kappa_z$ is the motility Péclet number, based on the maximum vertical swimming speed w_s. The beta function $\beta(\frac{1}{2}, \frac{1}{2}Pe_{swim})$ decreases monotonically with increasing Pe_{swim}. If $Pe_{swim} \gg 1$ ($\ll 1$) the layer thickness is much smaller (greater) than δ. Thus, as predicted by the scaling above, $H_e \sim \kappa_z/w_s$, layer thickness decreases with faster swimming speeds (**Figure 3d**) and weaker vertical dispersion.

3.3. Buoyancy

Even nonmotile phytoplankton can actively control their vertical position in the water column by regulating their buoyancy (i.e., their density difference with the ambient water). A number of mechanisms are employed, including gas vacuoles (Walsby 1972), carbohydrate ballasting

(Villareal & Carpenter 2003), and active replacement of ions in the internal sap (Gross & Zeuthen 1948). The density of marine phytoplankton typically lies in the range $\rho_p = 1.03\text{–}1.20$ g cm^{-3} for both motile and nonmotile species (Eppley et al. 1967, Kamykowski et al. 1992, Van Ierland & Peperzak 1984). While the settling velocity of motile cells can typically be neglected, as they swim much faster than they sink (Kamykowski et al. 1992), for nonmotile cells buoyancy represents an important means to move relative to the fluid. Similar to their motile counterparts, some nonmotile species also perform periodic vertical migrations by modulating their buoyancy. For example, the diatom *Rhizosolenia* completes a vertical migration cycle every 3–5 days (Richardson et al. 1998), and there is evidence that colonies of the nonmotile cyanobacterium *Trichodesmium* perform vertical migrations to great depths (potentially >100 m) on a daily basis (White et al. 2006).

Given phytoplankton's minute size (~1–1,000 μm) and small density contrast with seawater (typical seawater densities are $\rho_o = 1.02\text{–}1.03$ g cm^{-3}), their movement by buoyancy occurs at low Reynolds numbers. The Reynolds number, $Re = W_s D/\nu$, expresses the relative importance of inertial and viscous forces, where W_s is the vertical (settling or rising) speed relative to the fluid, D is a characteristic linear dimension of the cell, and ν ($\approx 1 \times 10^{-6}$ m^2 s^{-1}) is the kinematic viscosity of seawater. W_s is determined by the balance of gravitational force, buoyancy, and drag. For a spherical cell at $Re \ll 1$, $W_s = \Delta\rho g D^2/(18\rho_o\nu)$, where $\Delta\rho = \rho_p - \rho_o$ and g is the gravitational acceleration (Clift et al. 1978). Phytoplankton cells thus sink or rise unless their density is the same as that of the ambient fluid.

Buoyancy can therefore drive layer formation in a stratified water column [i.e., $\rho_o = \rho_o(z)$, Alldredge et al. 2002], when phytoplankton sink or rise to their depth of neutral buoyancy, z_o (where $\Delta\rho = 0$) (**Figure 2c**). Assuming that the fluid density increases linearly with depth (i.e., $d\rho_o/dz$ is constant), the density difference between the cell and the fluid is $\Delta\rho = -\rho_o N^2(z - z_o)/g$, where the buoyancy frequency is given by $N = [(g/\rho_o)d\rho_o/dz]^{1/2}$. One can use this to rewrite the buoyancy velocity as a function of the distance $z - z_o$ of a cell from its neutral buoyancy depth; i.e., $W_s(z) = -N^2 D^2(z - z_o)/(18\nu)$ (Stacey et al. 2007).

The spatiotemporal distribution of cells is governed by the same advection-diffusion equation introduced for convergent swimming (Equation 1), with the velocity $W(z)$ replaced by the buoyancy velocity $W_s(z)$. We note that this formulation assumes that N is constant over the depth of the layer, which may not hold exactly in practice but can often be considered a good first approximation. A scaling analysis yields the characteristic steady-steady thickness, $H_e \sim [18\nu\kappa_z/(N^2 D^2)]^{1/2}$, of a phytoplankton layer formed under the influence of buoyancy and turbulent dispersion (Stacey et al. 2007). Birch et al. (2009) calculated the steady-state distribution of cells,

$$c_e(z) = P\sqrt{\frac{\gamma}{2\pi\kappa_z}} \exp\left[-\frac{\gamma(z - z_o)^2}{2\kappa_z}\right], \qquad (3)$$

where P is the depth-integrated phytoplankton concentration and $\gamma = N^2 D^2/18\nu$. Thus steady-state profiles are Gaussian, with larger cells producing more compact layers (**Figure 3f**) owing to their higher vertical velocities. Solutions of the unsteady advection-diffusion equation reveal that for large cells, layer formation can occur within several hours (**Figure 3e**).

3.4. Gyrotactic Trapping

Thin layers are frequently found at depths at which the vertical shear is enhanced, in many cases corresponding to the location where the horizontal velocity changes direction (Cowles 2004, Dekshenieks et al. 2001, Ryan et al. 2008, Sullivan et al. 2010a). Vertical shear is often most pronounced at pycnoclines (Johnston & Rudnick 2009), where density stratification dampens

turbulence and suppresses overturning instabilities. Durham et al. (2009) proposed that vertical gradients in shear trigger the formation of thin layers of motile phytoplankton by disrupting their vertical migration. To perform vertical migration, motile phytoplankton swim in a direction parallel to that of gravity, via a mechanism known as gravitaxis (or geotaxis). Multiple processes can result in gravitaxis (Kessler 1985, Lebert & Häder 1996, Roberts & Deacon 2002), but all generate a stabilizing torque on the cell that acts to keep its swimming direction oriented along the vertical. However, when there is ambient flow, shear exerts a viscous, destabilizing torque on the cell, which tends to make it rotate. The swimming direction is set by the balance of the gravitactic and the viscous torques, and the cell is said to be gyrotactic (Kessler 1985). The susceptibility of a cell to shear, i.e., how easily the cell is rotated away from its vertical equilibrium orientation, is measured by the gyrotactic reorientation parameter, B, the timescale required for a cell in a quiescent fluid to return to its equilibrium orientation after being perturbed. Cells with larger B are more susceptible to being reoriented by shear.

Durham et al. (2009) showed that thin layers form at depths where the shear rate, S, exceeds a critical value, $S_{CR} = B^{-1}$. There are two distinct regimes of gyrotaxis: an equilibrium regime and a tumbling regime. In the equilibrium regime, the local shear rate is lower than the critical shear rate $[|S(z)| < S_{CR}]$, and a cell can reach its equilibrium orientation, given by $\sin\theta = BS$, where θ is the angle between the swimming direction and the vertical direction. In the tumbling regime, the shear rate exceeds the threshold $[|S(z)| > S_{CR}]$: the maximum stabilizing torque due to gravity is not sufficient to balance the destabilizing torque due to shear, causing the cell to tumble end over end. A tumbling cell has no vertical movement, as it remains trapped at the depth at which $|S(z)| = S_{CR}$. B is known only for a handful of species (Drescher et al. 2009, Durham et al. 2009, Hill & Häder 1997, Kessler 1985) and we estimate that it generally falls in the range 1–100 s.

When vertically migrating phytoplankton encounter increasing levels of shear, the vertical projection of their swimming speed, W, progressively decreases (because $\sin\theta = BS$). When cells reach the depth at which $|S(z)| = S_{CR}$, their upward speed vanishes ($W = 0$), leading to a gradient in cell flux and thus an accumulation of cells (**Figure 2d**). Durham et al. (2009) demonstrated in a laboratory experiment that this mechanism, which they termed gyrotactic trapping, drives layer formation. Motile phytoplankton were injected into a flow whose shear rate increased linearly with height. Using video microscopy, they detected intense thin layers at mid-depth in the device, for both the green alga *Chlamydomonas nivalis* and the toxic raphidophyte *H. akashiwo*. These observations were supported by tracking individual cells, which revealed the transition from the equilibrium regime to the tumbling regime, at a depth corresponding to S_{CR}. An individual-based numerical model successfully reproduced the salient features of the observations.

Similar to convergent swimming and buoyancy, gyrotactic trapping can be modeled with a one-dimensional advection-diffusion equation (Durham et al. 2009). To model the peak in shear often associated with thin phytoplankton layers, a representative fluid velocity profile $u(z) = -u_o\tanh[(z-z_o)/\delta]$ was used, in which the horizontal flow velocity $u(z)$ varies smoothly from u_o to $-u_o$ over a vertical distance on the order of δ. The corresponding shear rate is $S(z) = du/dz = -(u_o/\delta)\text{sech}^2[(z-z_o)/\delta]$, where z_o is the depth of zero fluid velocity and maximum shear. Combining this expression for $S(z)$ with the equilibrium orientation $\sin\theta = BS$ yields the vertical projection of the swimming speed, $W(z) = -w_{max}\{1-\Psi^2\,\text{sech}^4[(z-z_o)/\delta]\}^{1/2}$, where w_{max} is the vertical swimming speed when $S = 0$ and $\Psi = Bu_o/\delta$ is the plankton stability number. For depths z at which $|S(z)| > S_{CR}$ (tumbling regime), $W(z) = 0$ (Durham et al. 2009). The advection-diffusion equation for gyrotactic trapping is the same as that for convergent swimming and buoyancy (Equation 1), except that the vertical velocity is replaced by the expression for $W(z)$ derived here.

Turbulent dispersion acts to broaden the layer thickness as with the previous cases. The layer dynamics are governed by two dimensionless parameters: the plankton stability number, Ψ, and

the gyrotactic Péclet number, $Pe_{gyro} = w_{max}\delta/\kappa_z$. A first criterion for layer formation is $\Psi \gtrsim 1$; i.e., the shear rate must be large enough to stifle vertical migration. A second criterion is $Pe_{gyro} > 1$: Motility must bring cells into the region of enhanced shear faster than turbulent dispersion transports them through it.

Cells trapped in a high-shear region will eventually escape from the layer via turbulent dispersion. Once clear of the region where $|S(z)| > S_{CR}$, previously trapped cells can resume upward migration. Thus, similar to patch straining, thin layers produced via gyrotactic trapping are inherently transient: No steady-state distribution is attained because the supply of phytoplankton swimming into the layer is finite, and turbulent dispersion makes the layer leaky. The diel cycle of phytoplankton motility, the magnitude of turbulent dispersion, and the temporal coherence and vertical extent of the region of enhanced shear all likely affect the lifetime of a layer produced by this mechanism. Modeling suggests that layers produced via gyrotactic trapping could persist for more than 12 hours (**Figure 3g**).

Unlike patch straining, convergent swimming, and buoyancy—all of which generate layers that are symmetric about the depth of maximum concentration when the eddy diffusivity is constant over depth—gyrotactic trapping produces layers that are inherently asymmetric. The side of the layer where cells swim into the region of enhanced shear (the lower side in **Figure 3g,h**) features a considerably steeper gradient in cell concentration (larger $|dc/dz|$) than the opposite side. Furthermore, this mechanism predicts that species with different B will aggregate into spatially distinct layers, each corresponding to the depth of that species' critical shear rate (**Figure 3h**).

3.5. In Situ Growth

Layer formation via in situ growth can occur when growth is most vigorous at mid-depth— for example, when growth is either light- or nutrient-limited except over a small depth interval (**Figure 2e**) or when nutrients are abundant only at mid-depth (see Section 3.6). Consistent with the latter scenario, Birch et al. (2008) gave a detailed analysis of phytoplankton growth within a nutrient patch strained by shear, finding that the resulting layer dynamics largely follow the scalings for a phytoplankton patch in shear (see Section 3.1).

Growth is typically modeled using the differential equation $dc/dt = \mu_{net}c$, where μ_{net} is the net growth rate (growth minus mortality), yielding an exponential increase in phytoplankton or chlorophyll concentration over time. For the purpose of comparing with observations, this differential growth model is often approximated as $\Delta c = \mu_{net}c_0\Delta t$, where c_0 is the initial concentration and Δt the elapsed time (Steinbuck et al. 2010). Typical growth rates of phytoplankton range from $\mu = 0.4$ per day in polar habitats to $\mu = 0.7$ per day in tropical habitats, whereas grazing-induced mortality rates range from $r = 0.2$ per day to $r = 0.5$ per day in the same regions, respectively (Calbet & Landry 2004).

3.6. Intrusions

Intrusions can generate layers through the lateral transport of phytoplankton- or nutrient-rich waters into adjacent waters: The former produces thin layers directly (**Figure 2f**), whereas the latter produces layers by locally enhancing growth rates at mid-depth (see Section 3.5). Although several mechanisms can trigger intrusions, we focus on two general types of intrusion that have been implicated in layer formation: gravity-driven flows by salt wedge dynamics in estuaries (Kasai et al. 2010) and boundary mixing (Armi 1978, Phillips et al. 1986).

Estuaries often harbor phytoplankton blooms that result from the mixing of saltwater, containing nutrient-limited marine phytoplankton, with nutrient-replete freshwater (Nixon 1995). In salt wedge estuaries, the boundary between fresh riverine waters and the salty marine waters

intruding beneath them is especially sharp, because stratification suppresses vertical mixing. This boundary, where marine species mix with nutrient-rich waters (e.g., containing high nitrogen concentrations), often harbor thin layers, such as those observed in the Yura Estuary in Japan (Kasai et al. 2010). Two mechanisms are believed to have contributed to the formation of these layers: the upstream transport of phytoplankton-rich waters by the salt wedge intrusion and the diffusion of nutrient-rich freshwater through the interface between freshwater and saline water, which fuels growth (Kasai et al. 2010). The latter mechanism was supported by the observation that phytoplankton concentrations in the layer were higher than at the estuary's mouth, where the phytoplankton-rich water originated.

A second type of intrusion occurs when mixing along land boundaries interacts with stratification to drive offshore flows at the pycnocline (Armi 1978, Phillips et al. 1986). Several processes can induce boundary mixing, including breaking internal waves on sloping shores (McPhee-Shaw 2006), flow around islands (Simpson et al. 1982), and topographically influenced fronts (Pedersen 1994). The latter two have been observed to trigger layer formation by locally bolstering growth at mid-depth. In the first case, mixing induced by flow about the Scilly Isles in the Celtic Sea was observed to drive nitrate-rich waters from the deep sea into the well-lit pycnocline, producing layers composed of motile cells whose chlorophyll concentration was more than 15 times larger than ambient (Simpson et al. 1982). In the second case, a tidal front that occurred over Dogger's Bank in the North Sea interacted with the sloping bottom to drive a horizontal intrusion of water from the deeper depths into the thermocline. The resulting phytoplankton layers contained chlorophyll concentrations up to 20-fold larger than ambient (Pedersen 1994).

Boundary mixing has also been implicated in the direct formation of thin layers via offshore-directed intrusions of phytoplankton-rich waters. This mechanism was proposed by Steinbuck et al. (2010) to explain the formation of layers in the Gulf of Aqaba. Large intrusions are affected by hydrodynamic instabilities induced by Earth's rotation, which produce horizontal mixing with a dispersion coefficient $\kappa_{in} \approx 0.13 \; g'h/f$ (Ivey 1987), where h is the intrusion thickness, f is the Coriolis parameter, $g' = 0.07g(\rho_2 - \rho_1)/\rho_1$, and ρ_1 and ρ_2 are the water densities above and below the intrusion, respectively. With this formulation, Steinbuck et al. (2010) estimated the time, $t_{in} \approx L_{in}^2/(2\kappa_{in})$ (Fischer et al. 1979), required for an intrusion to propagate a distance L_{in}, finding good agreement with their observations. As the tongue of intruding water advances, vertical turbulent dispersion homogenizes it with the surrounding water, and the layer thickness increases as $H' \approx (2\kappa_z t_{in})^{1/2}$ (Fischer et al. 1979). These observations are discussed in more detail in Section 4.

3.7. Differential Grazing

Some zooplankton predators exhibit reduced grazing rates in regions that contain toxic or otherwise unpalatable species (Turner & Tester 1997), sometimes avoiding those species altogether (Bjornsen & Nielsen 1991, Nielsen et al. 1990). The prominence of a thin layer containing such phytoplankton species might be dramatically enhanced when zooplankton graze on other species above and below the layer. Although this mechanism does not per se create a thin layer, as species benefitting from reduced predation must first form a layer by another mechanism, differential grazing can increase a layer's chlorophyll signal relative to the surrounding waters, making layers of certain species detectable as surrounding species are consumed.

3.8. A Cautionary Note About Turbulent Dispersion

A note is in order regarding the role of turbulence, as it has been repeatedly suggested that vertical gradients in eddy diffusivity cause phytoplankton layers, by the accumulation of cells at depths

where diffusivity is low (e.g., pycnoclines; for examples, see Visser 1997). This proposition is based on an incorrect implementation of individual-based models. Properly formulated models, as well as solutions of the diffusion equation, demonstrate that—in the absence of a process that transports cells relative to the fluid (e.g., motility, buoyancy)—randomly distributed cells cannot form aggregations, even if turbulent dispersion is spatially variable (Ross & Sharples 2004, Visser 1997).

4. DEDUCING MECHANISMS OF LAYER FORMATION FROM FIELD OBSERVATIONS

Quantitative understanding of the physical and biological processes that mediate layer formation holds great promise for guiding field observations and for developing mathematical models to predict the occurrence and ecologically relevant characteristics of thin layers. In this section, we draw on the results of Section 3 to review recent reports of thin phytoplankton layers that applied quantitative methods to probe the mechanisms responsible for layer formation. The melding of theory and field observations pursued in these studies constitutes an important step toward a deeper understanding of thin layer dynamics.

4.1. Balancing Convergence and Turbulence Dispersion

One method to infer the mechanism driving the convergence of phytoplankton into a thin layer is to determine the properties of the cells or patches of cells required to counteract the vertical spreading of the layer caused by turbulent dispersion. Although this approach does not establish any direct causal relationships, it can help determine candidate mechanisms. Stacey et al. (2007) applied this method to four thin layers observed at pycnoclines in East Sound (Dekshenieks et al. 2001), for which they considered two convergence mechanisms: buoyancy and patch straining. Mechanisms invoking motility were not considered, because layers were mostly comprised of the diatom *Pseudo-nitzschia*, which is nonmotile. Using the measured layer thickness, eddy diffusivity, shear rate, and buoyancy frequency associated with each layer, Stacey et al. (2007) computed the cell diameter $D \sim (18 \nu \kappa_z / N^2 H_e^2)^{1/2}$ (see Section 3.3) required to generate the observed convergence by buoyancy and found it to agree remarkably well with independent measurements of the diameter. They also computed the layer tilt angle $\theta \sim (\kappa_z / S_u L_o^2)^{1/3}$ predicted if the layer had formed by straining (see Section 3.1 and **Figure 2a**), under the assumption that thinning by shear had reached a quasi-steady equilibrium with vertical dispersion, as expected at the time of minimum layer thickness (see Section 3.1). The predicted tilt angles also yielded plausible results, but a direct comparison was not possible because θ was not measured in the field. Thus both mechanisms were found to be consistent with observations, and neither could be ruled out as the culprit of layer formation.

A similar analysis was performed by Steinbuck et al. (2009) for thin layers of the dinoflagellate *A. sanguinea* (synonymous with *Gymnodinium sanguinea*) observed at the nutricline in Monterey Bay. *A. sanguinea* is highly motile (Park et al. 2002) and performs daily vertical migrations. Cells were found to begin swimming from the surface down to the nutricline 5–6 h before sunset and to aggregate there (Ryan et al. 2010, Sullivan et al. 2010a). Chlorophyll profiles acquired over 35 min during the afternoon showed that the population formed a thin layer at the thermocline, where turbulent dispersion had a local minimum (**Figure 4a,b**). The layer was highly asymmetric, with the magnitude of the concentration gradient $|\partial c / \partial z|$ below the peak being twice as large as above. This likely resulted from differences in turbulent dispersion, as the upper part of the layer
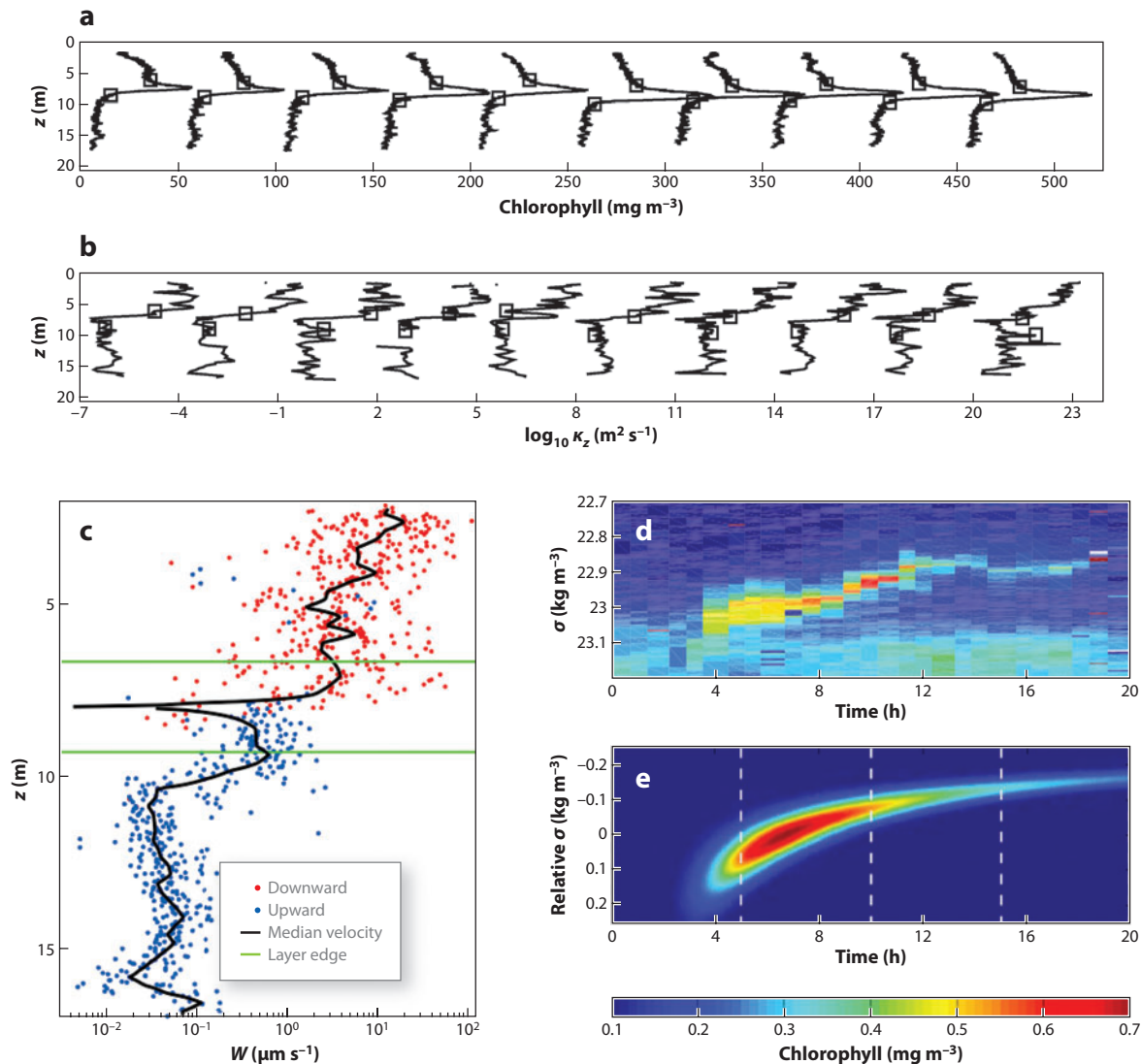
Figure 4

The use of mathematical models to interpret field observations provides insight into the processes that shape layer formation. (*a*–*c*) To maintain a steady phytoplankton distribution in the face of turbulent dispersion, a convergence mechanism must balance the spreading of the layer by turbulence. Using 10 high-resolution profiles of (*a*) the vertical distribution of chlorophyll and (*b*) the vertical eddy diffusivity acquired over a 35-min period in Monterey Bay, Steinbuck et al. (2009) estimated the local swimming velocity $W(z)$ required to balance turbulent dispersion. The median of $W(z)$ is shown by the black line in panel *c*. The edges of the layer are denoted by squares in panels *a* and *b* and by green lines in panel *c*. Vertical turbulent dispersion was larger above than below the layer, resulting in large inferred downward velocities above the layer ($W \sim 10 \ \mu\text{m s}^{-1}$) and small inferred upward velocities below the layer ($W \sim 0.1 \ \mu\text{m s}^{-1}$) (see Section 4). Sequential profiles are offset by 50 mg m^{-3} in panel *a* and by three decades in panel *b*. (*d,e*) Thin layers do not occur only in shallow coastal waters. (*d*) A thin layer observed by Hodges & Fratantoni (2009) in the Philippine Sea, where the total water depth exceeds 5,000 m. The layer exhibited a chlorophyll distribution that was tilted across lines of constant density (measured here in terms of the sigma-theta density, σ), a feature of layers formed via straining. (*e*) A simple model of straining successfully reproduces the basic characteristics of the layer. Panels *a*–*c* adapted with permission from Steinbuck et al. (2009); panels *a* and *b* copyright © 2009 by the American Society of Limnology and Oceanography Inc., panel *c* redrawn using data provided by the authors. Panels *d* and *e* adapted with permission from Hodges & Fratantoni (2009), copyright © 2009 by the American Geophysical Union.

extended into the energetic surface mixed layer ($\kappa_z \sim 10^{-5}$–10^{-4} m² s⁻¹), whereas the lower part experienced weaker turbulence ($\kappa_z \sim 10^{-6}$ m² s⁻¹).

Steinbuck et al. (2009) assumed that these layers were in steady state, with either cell motility or cell buoyancy balancing turbulent dispersion. This balance between convergence (by motility or buoyancy) and divergence (by turbulence) is expressed by the steady-state advection-diffusion equation (see Equation 1),

$$\frac{\mathrm{d}(c\,W)}{\mathrm{d}z} = \frac{\mathrm{d}}{\mathrm{d}z}\left(\kappa_z \frac{\mathrm{d}c}{\mathrm{d}z}\right). \qquad (4)$$

From this, one can infer the vertical convergence velocity, $W(z)$, required at each depth z to balance turbulent dispersion. Equation 4 yields $\ln(c/c_o) = \int(W/\kappa_z)\mathrm{d}z$ and, by differentiation, $W(z) = \kappa_z\,\mathrm{d}[\ln(c/c_o)]/\mathrm{d}z$, where c_o is the maximum cell concentration. This expression, combined with high-resolution measurements of κ_z, was used by Steinbuck et al. (2009) to determine the convergence velocity $W(z)$ required to produce the observed concentration profiles, c/c_o.

Because of its larger vertical eddy diffusivity κ_z, the region above the layer was found to require a much faster convergence velocity ($W \sim 10$ μm s⁻¹) than the region below the layer ($W \sim 0.1$ μm s⁻¹) (**Figure 4c**). Although sinking speeds of *A. sanguinea* can be of this order (≈ 20 μm s⁻¹; Kamykowski et al. 1992), layer formation by buoyancy was ruled out because gradients in fluid density were too weak: Measurements of the buoyancy frequency N showed that the settling velocity would have changed by only 1% over the depth of the layer, insufficient to explain observed accumulations. Instead, thin layers were consistent with an accumulation by convergent swimming, as this species' 300 μm s⁻¹ swimming speed (Park et al. 2002) was more than sufficient to account for the inferred velocities W.

To determine the time required for layer formation, Steinbuck et al. (2009) solved the unsteady advection-diffusion equation (Equation 1) using the inferred vertical swimming velocity profile for $W(z)$ (**Figure 4c**). Equation 1 was then integrated in time until the predicted vertical profile converged to the measured profile [convergence was guaranteed because the steady version of the same equation had been used to find $W(z)$]. The computed layer-formation time of 6 days was much longer than the measured time of a few hours, suggesting that $W(z)$ had been considerably higher during layer formation. Imposing a uniform downward swimming velocity of 20 μm s⁻¹ yielded the correct formation times (Sullivan et al. 2010a), but much thinner layers than were observed. Furthermore, independent estimates showed that vertical migration velocities were more than one order of magnitude larger (~ 240 μm s⁻¹) (Sullivan et al. 2010a).

Steinbuck et al. (2009) used the same method to rule out enhanced growth as the sole mechanism responsible for the formation of those layers. By solving the steady advection-diffusion equation balancing growth and turbulent dispersion, they computed the net growth rate, $\mu_{net}(z)$, necessary to counteract dispersion at each depth z, such that the predicted concentration profile matched the observed one. Net mortality ($\mu_{net} < 0$) was inferred on either side of the peak and net growth ($\mu_{net} > 0$) along the layer's centerline, the latter occurring at a rate that exceeded the maximum growth rate recorded for *A. sanguinea* (Doucette & Harrison 1990). In addition, the unsteady advection-diffusion equation predicted a layer-formation time 30-fold larger than measured, providing further support against layer formation via enhanced growth.

4.2. Fitting to an Ideal Distribution

Prairie et al. (2011) applied a similar technique to estimate the convergence strength, with one difference: They assumed that in the absence of turbulent dispersion, the phytoplankton distribution, $c(z)$, tends to an ideal distribution, $c^*(z)$, with finite thickness of H_T. H_T is a characteristic

of the underlying convergence process and represents a lower bound for the layer thickness. In contrast, in some convergence models layers would be infinitely thin in the absence of turbulence (e.g., convergent swimming, buoyancy, and gyrotactic trapping; see Section 3). Prairie et al. (2011) developed a framework to determine H_T and q, the rate at which $c(z)$ tends to $c^*(z)$, by fitting measured vertical gradients of phytoplankton abundance. Using 30-cm segments from seven high-resolution phytoplankton profiles collected in the Santa Barbara Channel, they found $H_T \sim 1$ m and $q = 0.5$–0.9 per day. The latter values are in line with maximal growth rates of *Pseudo-nitzchia*, the dominant genus during the observations (Prairie et al. 2010), suggesting that enhanced growth within 1-m-thick regions of the water column could have formed the observed layers (though other mechanisms, such as buoyancy, could not be ruled out). By providing information on thickness and rate of convergence, this approach represents a useful addition to the tools that can be applied to identify mechanisms of layer formation.

4.3. Quantifying Changes in Layer Thickness

Another approach to infer convergence mechanisms is based on the quantification of the rate of change of layer thickness, dH/dt. This was done by Cheriton et al. (2009) for 99 profiles of a thin layer of *A. sanguinea* collected over an 8.5-h nighttime period in Monterey Bay. They compared the mean observed rate of change, $(dH/dt)_{obs} \approx -2$ mm s^{-1}, with the rates of layer convergence predicted for buoyancy, straining, and motility. Following the scaling analysis of Stacey et al. (2007), Cheriton and coworkers computed the convergence rates as $(dH/dt)_{sink} \approx w_2 - w_1 \approx -0.3$ μm s^{-1} for sinking (where w_1 and w_2 are the sinking speeds at the upper and lower boundaries of the layer, calculated using the local fluid density; see Section 3.3); $(dH/dt)_{strain} \approx -H/\Delta t \approx -60$ μm s^{-1} for straining (where Δt is the time since the onset of patch straining and the tilt angle is assumed to be small); and $(dH/dt)_{swim} \approx -2w_s \approx -600$ μm s^{-1} for convergent swimming. All three predicted rates were considerably smaller in magnitude than $(dH/dt)_{obs}$, suggesting that none of these mechanisms produced the layer.

Yet further inspection revealed that internal waves produced oscillatory contractions and expansions of isopycnals (surfaces of constant density), greatly increasing the apparent, instantaneous dH/dt (Cheriton et al. 2009). This internal-wave-driven thinning and thickening is a transient and reversible process (Franks 1995, Stocker & Imberger 2003). After removing it, by calculating dH/dt relative to isopycnals, Cheriton et al. (2009) found that straining and sinking were still too weak and that only swimming could have produced the observed convergence rates. However, we note that this treatment omits the effect of turbulent dispersion: $(dH/dt)_{obs}$ did not result solely from the convergence mechanism, but from the competition between the convergence mechanism and turbulent dispersion, casting some doubt on the validity of this approach to infer convergence mechanisms. For example, including dispersion would further increase the required rate of layer convergence (Steinbuck et al. 2009), implying that even swimming might not have been sufficient to produce the layer.

4.4. Case Studies: Inferring Convergence Mechanisms from Systematic Analysis

A systematic and insightful analysis of possible mechanisms of layer formation, providing a template for future studies, was presented by Steinbuck et al. (2010). These authors investigated thin layers, likely dominated by the cyanobacteria *Prochlorococcus* and *Synechococcus*, observed 1.6 km offshore in the Gulf of Aqaba. Patch straining was excluded because the required initial patch length $L \sim (H_{min})^3 S_u / \kappa_z \sim 10^2$–$10^4$ km (see Section 3.1)—calculated using parameters measured in situ—was much larger than could be contained in the narrow bay (<10 km). The swimming

speeds required to balance turbulent dispersion, $w_s \sim \kappa_z / H_e$ (see Section 3.2), were small ($\sim$0.1–1 μm s^{-1}) and easily achieved by the motile clade of *Synechococcus*. However, dividing the layer's excess concentration, Δc (relative to the surrounding concentration c_{ext}), by the flux of cells due to swimming, $w_s c_{ext}$, yielded a timescale of layer formation, $H_e \Delta c / (w_s c_{ext}) \sim$ 10–100 days, much larger than was observed (<1 day). Buoyancy was also excluded because the cell diameter required to compensate turbulent dispersion, $D \sim (18 \nu \kappa_z / N^2 H_e^2)^{1/2} =$ 50–400 μm (see Section 3.3), was much larger than the <5-μm size of the cyanobacteria.

Near the shore, chlorophyll concentrations were similar to those found in the layers, suggesting that layers were formed by intrusions. To test this hypothesis, Steinbuck and coworkers integrated the horizontal fluid velocity at the depth of the layers backward in time to estimate the path of the water before it arrived at the sampling location. Thin layers were observed when water originated from the shoreward direction, whereas no layers formed when water originated from offshore. The thickness and intrusion time of the layers were successfully compared to theoretical predictions. The time required to propagate the distance from shore, $L_{in} =$ 1.6 km, was computed to be $t_{in} \approx L_{in}^2 / (2 \kappa_{in}) \approx$ 5–20 h (see Section 3.6), in good agreement with estimates obtained from the integration of horizontal velocities. The predicted increase in layer thickness with time, $H' \approx (2 \kappa_z t_{in})^{1/2} \approx$ 6–10 m (see Section 3.6), was also consistent with observations, indicating that turbulent dispersion would not completely dissipate the intruding high cell concentrations before they reached the sampling location.

In one of the few thin phytoplankton layer recordings made in the open ocean, Hodges & Fratantoni (2009) used autonomous gliders to sample a layer located 800 km east of the Luzon Strait, in $\approx$5,000-m water depth. A patch of low-salinity, high-chlorophyll water was advected across the 100 $\times$ 100 km^2 sampling area, at a depth of 100 m, $\approx$40 m above the deep chlorophyll maximum. The layer was observed simultaneously by two gliders separated by 75 km, implying that it extended for at least this distance. Over a 16-h period, the layer thickness decreased from 20 to 2 m. This coincided with the thinning of the low-salinity lens, indicating that cells were not actively moving relative to the flow. As it thinned, the layer tilted across isopycnals, consistent with patch straining (see Section 3.1). The shear required to strain the patch was likely provided by the diurnal internal waves observed during the study. Hodges & Fratantoni (2009) developed a model of layer formation via patch straining similar to that of Birch et al. (2008) but neglecting turbulent dispersion, which gave good agreement with their observations (**Figure 4d,e**).

The formation of some layers appears to be driven by the interaction of cell motility and flow. Sullivan et al. (2010a) observed thin layers of the highly motile, toxic dinoflagellate *Alexandrium catenella* in Monterey Bay. No clear diel pattern was found, possibly because of confounding effects due to the simultaneous presence of nonmotile species (e.g., *Chaetoceros*) (Rines et al. 2010). Layers formed 1–2 m beneath peaks in shear, during both the daytime and nighttime. The shear rate averaged $S \approx 0.01$ s^{-1} at the center of the layers and peaked at $S \approx 0.03$ s^{-1} above the layers. Turbulence was also enhanced above the layers. Sullivan et al. (2010a) suggested that these layers might have formed as a result of modifications of the cells' swimming behavior. This hypothesis is supported by laboratory experiments in which shear was found to markedly affect *A. catenella*'s swimming behavior (Karp-Boss et al. 2000). Flow-induced changes in swimming are predicted by gyrotactic trapping, in which shear inhibits vertical motility by inducing phytoplankton tumbling, either through the mean flow (Durham et al. 2009) or via turbulence (Durham et al. 2011). Confirmation of this hypothesis, however, will require in situ observations of cell motility and knowledge of the cells' critical shear rate (B^{-1}) (see Section 3.4).

An interesting case is provided by the thin layers associated with a region of upwelling that occurred in Monterey Bay in 2003, independently observed by Ryan et al. (2008) and Johnston et al. (2009). Ryan et al. (2008) found that all layers occurred at the thermocline and that most (92%)

coincided with depths where ambient currents sharply changed direction over depth. Vertical shear profiles exhibited a strong peak that coincided with the center of the layers, and thinner layers were associated with higher shear rates. The layers' species composition was not determined, but cells did not exhibit vertical migration: The layer depth closely followed a single isotherm, indicating that cells were not moving relative to the fluid. Synoptic mapping revealed the presence of strong horizontal patchiness at 1–3-km scales before layers were observed. This patchiness, together with the observed correlation of layers with shear, led both Ryan et al. (2008) and Johnston et al. (2009) to suggest that layers had formed via patch straining. However, Johnston et al. (2009) noted that chlorophyll concentrations within the layers were larger than in the upwelled subsurface chlorophyll maxima from which the layers originated. This fact implies that a mechanism other than straining (e.g., in situ growth) determined or codetermined the formation of these layers, because straining cannot account for an increase in concentration compared to the original patch (see Section 3.1).

4.5. Concluding Remarks

We conclude this section by noting that, to date, identification of the mechanism driving the formation of a thin layer is rarely achieved by direct observation, but rather by using theoretical models to determine which mechanisms are capable of producing salient features of the layer and to rule out mechanisms with attributes that are incompatible with observations. It would be highly desirable to complement this deductive approach with novel observational techniques that directly characterize rates of layer convergence, permitting more definitive conclusions about the mechanisms of layer formation. For example, because thin layers can form as a result of phytoplankton motility, it will be important to develop techniques to quantify cell motility in situ. Such direct observations of biophysical marine processes are sorely needed to interpret field observations and inform predictive models. Furthermore, the overwhelming majority of thin layer observations have been made in coastal water bodies: Comprehensive studies in other locales, including the open ocean, would enable a broader understanding of the processes relevant to layer formation and a greater ability to test hypotheses on the role of thin layers in the instigation of HABs (see Section 2.9).

5. TROPHIC INTERACTIONS

Thin layers are a remarkable example of a heterogeneous distribution of primary producers. By concentrating large amounts of prey over small depth intervals, thin layers have the potential to induce predator aggregation and thus substantially increase trophic transfer rates compared with more homogeneous phytoplankton distributions (Cowles et al. 1998, Tiselius et al. 1993). Indeed, correlations between thin layers of phytoplankton and zooplankton are often observed (Benoit-Bird et al. 2009, 2010; Gallager et al. 2004; McManus et al. 2003; Menden-Deuer 2008; Menden-Deuer & Fredrickson 2010), although zooplankton avoidance of toxic and mucus-rich phytoplankton layers has also been reported (Alldredge et al. 2002, Bjornsen & Nielsen 1991, Nielsen et al. 1990).

An early, dramatic link between phytoplankton layers and higher trophic levels was demonstrated by Lasker (1975), who found that the feeding success of anchovy larvae in water collected from within a thin layer of *Gymnodinium sanguineum* (synonymous with *Gymnodinium splendens*) was dramatically greater than in water collected from the surface. Furthermore, larval feeding was negligible after a storm had destroyed the thin layer, likely because prey concentrations became too dilute. This finding is emblematic of a fundamental principle of planktonic life in the sea:

Resource densities are often too low for survival (e.g., Mullin & Brooks 1976), as summarized in the adage "the mean fish is a dead fish" (Preston et al. 2010). In this respect, Lasker's observations exemplify the critical role that thin layers can play in the sustenance of higher trophic levels and highlight their potential impact on the recruitment of fish larvae.

One strategy that predators use to enhance foraging when prey distributions are heterogeneous is to engage in area-restricted search behavior. In phytoplankton layers, this behavior can result from a number of predator adaptations, including altered swimming speeds, increased turning rates, and a bias of swimming in the horizontal direction (Tiselius 1992, Woodson et al. 2005). The ability of predators to exploit phytoplankton layers was demonstrated in experiments in which copepods (*Acartia tonsa*) were exposed to two different distributions of prey (*Thalassiosira weissflogii*) within a 20-cm-tall column (Tiselius 1992). In the first treatment, phytoplankton cells were distributed homogeneously over depth, whereas in the second treatment, they were confined to a 3-cm-thick layer, at the same concentration. Despite the total abundance of prey being more than six times larger in the homogeneous treatment, the grazing rates were very similar in the two cases owing to the copepods' ability to find and maintain their position within the layer (Tiselius 1992).

Herbivorous zooplankters likely use a variety of cues to locate thin phytoplankton layers. The use of chemical cues is demonstrated by the observation that grazers aggregate in patches of cell-free phytoplankton exudates (Menden-Deuer & Grünbaum 2006, Woodson et al. 2007). It has also been speculated that physical cues—including vertical gradients in fluid density and fluid velocity—might be used by predators as proxies to find thin layers. For example, grazers actively aggregate at pycnoclines (Harder 1968, Harvey & Menden-Deuer 2011) and engage in area-restricted search behaviors where shear is enhanced (Woodson et al. 2005, 2007): Both density gradients and velocity gradients are often associated with thin phytoplankton layers (see Section 2.7). Woodson et al. (2007) posited that such strategies allow predators to focus on regions of the water column more likely to contain prey. Harder (1968) observed that the copepod *Temora longicornis* aggregated at density gradients when there was no corresponding gradient in salinity but failed to aggregate in salinity gradients when there was no associated gradient in density, suggesting that copepods may actively seek pycnoclines using mechanical cues, as opposed to passively aggregating there in response to salt-induced stress.

Behavioral adaptations that allow grazers to aggregate within a thin phytoplankton layer are not without risk: Although this strategy confers increased foraging rates, it also exposes grazers to potentially higher mortality rates due to predation by higher trophic levels (e.g., larger zooplankton or fish). This trade-off has been analyzed using individual-based models of organisms foraging within patchy, layered prey landscapes (Tiselius et al. 1993). Two classes of grazers were simulated—ciliates and copepods—using functional responses, swimming speeds, and predation risks typical of each class. In the absence of predation by higher trophic levels, both classes of grazers benefitted from an area-restricted search behavior in terms of enhanced growth rates. However, when predation of grazers was included, ciliates achieved a higher net growth rate by adopting an area-restricted search behavior, whereas this strategy conferred only marginal advantages to copepods. These results indicate that, for copepods, accumulating to forage on thin phytoplankton layers is beneficial only under certain conditions. Consistent with these predictions, observations in East Sound revealed that thin phytoplankton layers were correlated with increased ciliate (and heterotrophic dinoflagellate) abundance, though it could not be ascertained whether these correlations occurred due to altered motility or enhanced predator growth rates (Menden-Deuer 2008).

With these general considerations as a background, we now focus on three field studies that provide a unique perspective on the relationship of thin phytoplankton layers with higher trophic
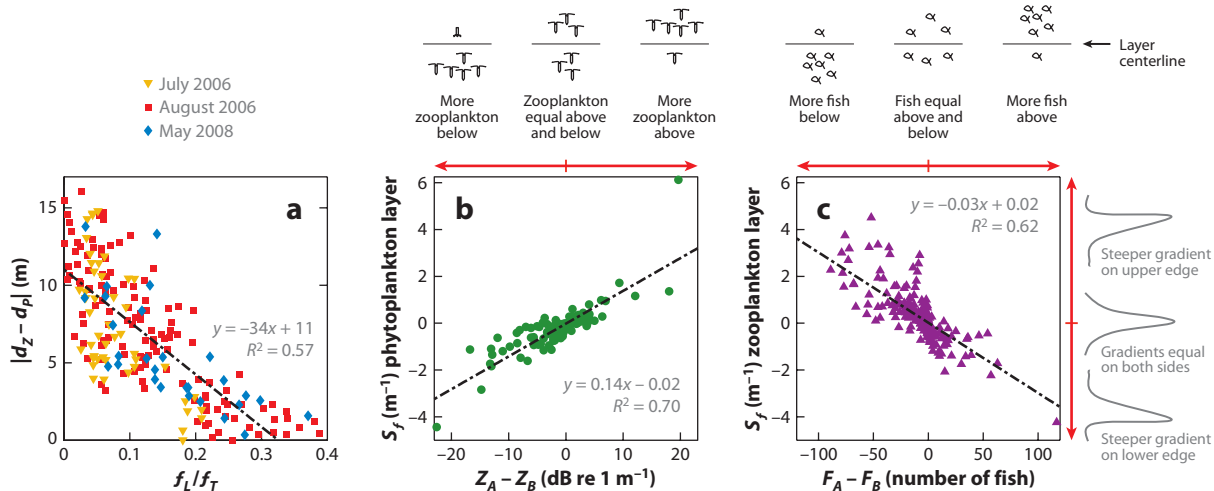
Figure 5

Thin phytoplankton layers are often correlated with the distribution of organisms from higher tropic levels, although the mechanisms behind these correlations remain largely unknown. (*a*) Benoit-Bird et al. (2010) measured the vertical distance $|d_Z - d_P|$ between the depth of the zooplankton layer d_Z and the depth of the phytoplankton layer d_P, over 11 nights in Monterey Bay. The distance was smaller when the fraction of chlorophyll in the phytoplankton layer, relative to the entire water column, f_L/f_T, was larger. This suggests that zooplankters scan the entire water column, aggregating near phytoplankton layers only when these are sufficiently concentrated. (*b,c*) Higher trophic levels can affect the vertical structure of thin layers of phytoplankton and zooplankton. Benoit-Bird et al. (2009) quantified the vertical asymmetry of thin layers by means of a shape factor, S_f, for thin layers observed in Monterey Bay. S_f measures the difference in the magnitude of the concentration gradient above and below the layer (e.g., $S_f > 0$ indicates that the gradient is sharper at the upper edge; see Section 5). The difference in the amount of predators above and below the layer is $Z_A - Z_B$ for zooplankton (on a logarithmic scale, in panel *b*) and $F_A - F_B$ for fish. The asymmetry in the shape of the phytoplankton layer is well predicted by the relative distribution of zooplankton (*b*). Similarly, the asymmetry in the shape of the zooplankton layer is well predicted by the relative distribution of fish (*c*). However, the two trends are opposite: The phytoplankton layer is steeper on the side with more zooplankton, whereas the zooplankton layer is steeper on the side with less fish. In all panels, the dashed black lines are least-squares regressions to the data. Panel *a* adapted with permission from Benoit-Bird et al. (2010), using data provided by the authors; panels *b* and *c* adapted with permission from Benoit-Bird et al. (2009), also using data provided by the authors.

levels. The first study is a detailed analysis of the correlations between vertical phytoplankton and zooplankton distributions during nighttime hours in Monterey Bay, recorded in 2006 and 2008 (Benoit-Bird et al. 2010). Both phytoplankton and zooplankton were observed to intermittently aggregate into layers. While the acoustic technique used to sample zooplankton layers does not readily permit organism identification, net tows found that 90% of the zooplankton biomass was composed of three copepod genera (*Calanus*, *Ctenocalanus*, and *Acartia*). Although the depth of the zooplankton layer and that of the phytoplankton layer were sometimes highly correlated, at other times they were up to 16 m apart. Whether phytoplankton and zooplankton layers were colocalized was independent of the phytoplankton layer's peak chlorophyll concentration and instead correlated with the fraction of chlorophyll contained within the layer (**Figure 5a**): For phytoplankton layers comprising >20% of the total chlorophyll in the water column, zooplankton layers were in close proximity. Although the mechanism that led to this correlation remains unknown, this analysis suggests that zooplankton can assess prey availability over the entire depth of the water column, likely through vertical migration. Conversely, it is interesting to note that the likelihood of a zooplankton layer occurring at any depth was independent of whether a thin phytoplankton layer was present. More broadly, this result shows that the trophic consequences of thin phytoplankton layers cannot be assessed without considering the distribution of

phytoplankton over the rest of the water column. Finally, it is tempting to draw a connection between these results and the aforementioned model of Tiselius et al. (1993): Might copepods expose themselves to higher predation risks only when their phytoplankton prey are highly aggregated, such that the payoff shifts the gamble in their favor?

The second study we focus on provides perhaps the only field measurement of grazing rates within thin layers, a crucial step towards quantifying the ecological interactions between phytoplankton and zooplankton in layers. Using samples collected from within and outside thin layers in East Sound, Washington, over three years, Menden-Deuer & Fredrickson (2010) performed laboratory dilution experiments to estimate in situ rates of phytoplankton growth and grazing, the latter limited to small (<200 μm) protistan grazers. Although the mechanisms responsible for layer formation were not identified, two conclusions could be reached. First, in situ growth was ruled out as the layer-formation mechanism, because phytoplankton growth rates were the same inside and outside layers ($\mu = 0.34$ per day). Second, most layers were short-lived (less than a few days) and average grazing rates were considerably higher inside layers ($r = 0.25$ per day) than outside ($r = 0.09$ per day). This is consistent with the hypothesis that layer persistence is curtailed by enhanced predation pressure: If grazing removes phytoplankton from a layer faster than convergent processes transport them into it, a reduction in the layer's intensity will occur.

The third study analyzes the effect of predation on the vertical structure of a thin layer. As we saw, gyrotactic trapping (see Section 3.4) and gradients in vertical eddy diffusivity lead to asymmetric layers (see Section 4), in which the concentration gradients $|\partial c/\partial z|$ above and below the layer differ. From data collected in Monterey Bay, Benoit-Bird et al. (2009) showed that such asymmetries can also result from the interaction with higher trophic levels for both phytoplankton and zooplankton layers. Layer asymmetry was quantified with a shape factor, $S_f = (|\partial s/\partial z|_{above} - |\partial s/\partial z|_{below})/\max(s)$, where s is the local abundance of the organism composing the layer. Normalization by the peak abundance, $\max(s)$, removed the influence of layer intensity. No correlation was found between S_f and differences in vertical shear above and below the layer, indicating that layer asymmetry was likely not associated with gyrotactic trapping or gradients in turbulent dispersion. Instead, S_f was well correlated with predator abundance, but, intriguingly, asymmetries in predator abundance showed the opposite trend in the two types of layers: Phytoplankton layers had a steeper gradient on the side where more zooplankters resided (**Figure 5b**), whereas zooplankton layers had shallower gradients on the side containing more fish (**Figure 5c**). Furthermore, in the absence of predators, thin layers of both types were more symmetric with 10-fold smaller S_f. While the mechanisms mediating these interactions remain unknown, the shape factor of both types of prey layers appear to be actively modulated by predators (Benoit-Bird 2009, Benoit-Bird et al. 2009), suggesting that layers did not result from predators' preference for a particular prey gradient. In summary, this study demonstrates how trophic interactions can be a driver of layer morphology and suggests that predators should be considered when assessing layer dynamics.

SUMMARY POINTS

1. Thin phytoplankton layers are recurrent features of the marine environment, observed mostly in the coastal ocean but recently also in open waters, that can harbor a considerable fraction of the water column's primary producers within small depth intervals.

2. Advanced sampling technologies and meticulous field campaigns have greatly increased our ability to quantify thin layer characteristics, dynamics, and accompanying environmental conditions.

3. Thin phytoplankton layers can form owing to diverse biophysical mechanisms, including cell behavior (e.g., motility, sensing), morphology (e.g., cell diameter, density, asymmetry), fluid flow (e.g., shear, intrusions), and population dynamics (e.g., cell growth, grazing rates). Each convergence mechanism produces distinctive layer characteristics and correlations with the biophysical environment that can help diagnose the processes at play in field observations.

4. Scaling analyses and mathematical models of layer formation have been applied to field observations to identify candidate mechanisms and rule out those that are incompatible. However, rarely have putative mechanisms been directly demonstrated.

5. Thin layers of toxic phytoplankton species may play an important role in instigating HABs.

6. As trophic hotspots, thin phytoplankton layers can play an outsized role in mediating the survival and reproduction rates of organisms belonging to higher trophic levels.

7. The predators of phytoplankton may have evolved behavioral adaptations to locate and exploit thin layers, yet the specific trade-offs that underlie observed correlations between the positions of thin phytoplankton layers and predator assemblages remain unknown.

FUTURE ISSUES

1. Broadening the scope of future field campaigns to new, diverse environments, including the open ocean and lakes, will test the universality of currently proposed mechanisms for layer formation.

2. Developing the next generation of mathematical models and scaling arguments that incorporate salient features of field observations will allow for a tighter coupling between models and observations.

3. The development of novel techniques that enable cell behavior to be observed in situ will allow direct testing and informed discrimination of layer-formation mechanisms.

4. New laboratory experiments can enable controlled tests of specific layer-formation processes, quantification of phytoplankton responses to imposed stimuli, and measurements of phytoplankton physiological and morphological parameters, especially as they pertain to motility.

5. The incorporation of the biophysical interactions that drive thin layer dynamics into models of HABs could enhance these models' predictive abilities and contribute to the development of bloom forecasting.

6. Understanding the trade-offs of residing in concentrated thin layers will provide a clearer ecological picture of the causes and consequences of thin layers.

7. Determining the processes that mediate the co-occurrence of thin phytoplankton layers, zooplankton layers, and fish will help assess impacts of thin layers on the marine food web.

DISCLOSURE STATEMENT

The authors are not aware of any affiliations, memberships, funding, or financial holdings that might be perceived as affecting the objectivity of this review.

ACKNOWLEDGMENTS

LITERATURE CITED

Alldredge AL, Cowles TJ, MacIntyre S, Rines JEB, Donaghay PL, et al. 2002. Occurrence and mechanisms of formation of a dramatic thin layer of marine snow in a shallow Pacific fjord. *Mar. Ecol. Prog. Ser.* 233:1–12

Armi L. 1978. Some evidence for boundary mixing in the deep ocean. *J. Geophys. Res.* 83:1971–79

Baek SH, Shimode S, Shin K, Han MS, Kikuchi T. 2009. Growth of dinoflagellates, *Ceratium furca* and *Ceratium fusus* in Sagami Bay, Japan: the role of vertical migration and cell division. *Harmful Algae* 8:843–56

Benoit-Bird KJ. 2009. Dynamic 3-dimensional structure of thin zooplankton layers is impacted by foraging fish. *Mar. Ecol. Prog. Ser.* 396:61–76

Benoit-Bird KJ, Cowles TJ, Wingard CE. 2009. Edge gradients provide evidence of ecological interactions in planktonic thin layers. *Limnol. Oceanogr.* 54:1382–92

Benoit-Bird KJ, Moline MA, Waluk CM, Robbins IC. 2010. Integrated measurements of acoustical and optical thin layers I: vertical scales of association. *Cont. Shelf Res.* 30:17–28

Birch DA, Young WR, Franks PJS. 2008. Thin layers of plankton: formation by shear and death by diffusion. *Deep-Sea Res. Part I* 55:277–95

Birch DA, Young WR, Franks PJS. 2009. Plankton layer profiles as determined by shearing, sinking, and swimming. *Limnol. Oceanogr.* 54:397–99

Bjornsen PK, Nielsen TG. 1991. Decimeter scale heterogeneity in the plankton during a pycnocline bloom of *Gyrodinium aureolum*. *Mar. Ecol. Prog. Ser.* 73:263–67

Bollens SM, Rollwagen-Bollens G, Quenette JA, Bochdansky AB. 2011. Cascading migrations and implications for vertical fluxes in pelagic ecosystems. *J. Plankton Res.* 33:349–55

Bracco A, Provenzale A, Scheuring I. 2000. Mesoscale vortices and the paradox of the plankton. *Proc. R. Soc. B* 267:1795–1800

Brahamsha B. 1999. Non-flagellar swimming in marine *Synechococcus*. *J. Mol. Microbiol. Biotechnol.* 1:59–62

Calbet A, Landry MR. 2004. Phytoplankton growth, microzooplankton grazing, and carbon cycling in marine systems. *Limnol. Oceanogr.* 49:51–57

Cheriton OM, McManus MA, Stacey MT, Steinbuck JV. 2009. Physical and biological controls on the maintenance and dissipation of a thin phytoplankton layer. *Mar. Ecol. Prog. Ser.* 378:55–69

Cheriton OM, McManus MA, Steinbuck JV, Stacey MT, Sullivan JM. 2010. Towed vehicle observations of thin layer structure and a low-salinity intrusion in Northern Monterey Bay, CA. *Cont. Shelf Res.* 30:39–49

Churnside JH, Donaghay PL. 2009. Thin scattering layers observed by airborne lidar. *ICES J. Mar. Sci.* 66:778–89

Clift R, Grace JR, Weber ME. 1978. *Bubbles, Drops, and Particles*. New York: Academic

Cowles TJ. 2004. Planktonic layers: physical and biological interactions on the small-scale. In *Handbook of Scaling Methods in Aquatic Ecology: Measurement, Analysis, Simulation*, ed. L Seuront, PG Strutton, pp. 31–49. Boca Raton, FL: CRC

Shows that the vertical structure of a thin layer can be affected by the relative distribution of predators above and below the layer.

Shows that zooplankton layers reside closer to phytoplankton layers when the latter contain a larger fraction of the water column's chlorophyll.

Provides a detailed theoretical analysis of layer formation via straining.

Cowles TJ, Desiderio RA, Carr ME. 1998. Small-scale planktonic structure: persistence and trophic consequences. *Oceanography* 11:4–9

Cullen JJ. 1982. The deep chlorophyll maximum: comparing vertical profiles of chlorophyll *a*. *Can. J. Fish. Aquat. Sci.* 39:791–803

Dekshenieks MM, Donaghay PL, Sullivan JM, Rines JEB, Osborn TR, Twardowski MS. 2001. Temporal and spatial occurrence of thin phytoplankton layers in relation to physical processes. *Mar. Ecol. Prog. Ser.* 223:61–71

Donaghay PL, Osborn TR. 1997. Toward a theory of biological-physical control of harmful algal bloom dynamics and impacts. *Limnol. Oceanogr.* 42:1283–96

Donaghay PL, Rines HM, Sieburth JM. 1992. Simultaneous sampling of fine scale biological, chemical, and physical structure in stratified waters. *Arch. Hydrobiol. Beih.* 36:97–108

Doucette GJ, Harrison PJ. 1990. Some effects of iron and nitrogen stress on the red tide dinoflagellate *Gymnodinium sanguineum*. *Mar. Ecol. Prog. Ser.* 62:293–306

Drescher K, Leptos KC, Tuval I, Ishikawa T, Pedley TJ, Goldstein RE. 2009. Dancing *Volvox*: hydrodynamic bound states of swimming algae. *Phys. Rev. Lett.* 102:168101

Durham WM, Climent E, Stocker R. 2011. Gyrotaxis in a steady vortical flow. *Phys. Rev. Lett.* 106:238102

Durham WM, Kessler JO, Stocker R. 2009. Disruption of vertical motility by shear triggers formation of thin phytoplankton layers. *Science* 323:1067–70

Eckart C. 1948. An analysis of the stirring and mixing processes in incompressible fluids. *J. Mar. Res.* 7:265–75

Eppley RW, Holmes RW, Strickland JDH. 1967. Sinking rates of marine phytoplankton measured with a fluorometer. *J. Exp. Mar. Biol. Ecol.* 1:191–208

Fauchot J, Levasseur M, Roy S. 2005. Daytime and nighttime vertical migrations of *Alexandrium tamarense* in the St. Lawrence estuary (Canada). *Mar. Ecol. Prog. Ser.* 296:241–50

Fenchel T. 2001. How dinoflagellates swim. *Protist* 152:329–38

Fischer HB, List EJ, Koh RCY, Imberger J, Brooks NH. 1979. *Mixing in Inland and Coastal Waters*. New York: Academic

Franks PJS. 1995. Thin-layers of phytoplankton: a model of formation by near-inertial wave shear. *Deep-Sea Res. Part I* 42:75–91

Franks PJS. 1997. Models of harmful algal blooms. *Limnol. Oceanogr.* 42:1273–82

Gallager SM, Yamazaki H, Davis CS. 2004. Contribution of fine-scale vertical structure and swimming behavior to formation of plankton layers on Georges Bank. *Mar. Ecol. Prog. Ser.* 267:27–43

Gentien P, Donaghay PL, Yamazaki H, Raine R, Reguera B, Osborn T. 2005. Harmful algal blooms in stratified environments. *Oceanography* 18:172–83

Gjosaeter J, Lekve K, Stenseth NC, Leinaas HP, Christie H, et al. 2000. A long-term perspective on the *Chrysochromulina* bloom on the Norwegian Skagerrak coast 1988: a catastrophe or an innocent incident? *Mar. Ecol. Prog. Ser.* 207:201–18

Gross F, Zeuthen E. 1948. The buoyancy of plankton diatoms: a problem of cell physiology. *Proc. R. Soc. Lond. Ser. B* 135:382–89

Grünbaum D. 2009. Peter principle packs a peck of phytoplankton. *Science* 323:1022–23

Guasto JS, Rusconi R, Stocker R. 2012. Fluid mechanics of planktonic microorganisms. *Annu. Rev. Fluid Mech.* 44:1–28

Harder W. 1968. Reactions of plankton organisms to water stratification. *Limnol. Oceanogr.* 13:156–68

Harvey EL, Menden-Deuer S. 2011. Avoidance, movement, and mortality: the interactions between a protistan grazer and *Heterosigma akashiwo*, a harmful algal bloom species. *Limnol. Oceanogr.* 56:371–78

Heil CA, Glibert PM, Fan CL. 2005. *Prorocentrum minimum* (Pavillard) Schiller: a review of a harmful algal bloom species of growing worldwide importance. *Harmful Algae* 4:449–70

Hill NA, Häder DP. 1997. A biased random walk model for the trajectories of swimming micro-organisms. *J. Theor. Biol.* 186:503–26

Hodges BA, Fratantoni DM. 2009. A thin layer of phytoplankton observed in the Philippine Sea with a synthetic moored array of autonomous gliders. *J. Geophys. Res.* 114:C10020

Holliday DV, Pieper RE, Greenlaw CF, Dawson JK. 1998. Acoustical sensing of small-scale vertical structures in zooplankton assemblages. *Oceanography* 11:18–23

Provides one of the first quantitative reports of thin layers and their associated physical environment, highlighting the intimate connection between the two.

Shows that thin layers can form when vertical migration is disrupted by fluid shear, a process called gyrotactic trapping.

Using sophisticated glider technology, shows that thin layers are not limited to the coastal ocean but can also occur in the open ocean.

Hutchinson GE. 1961. The paradox of the plankton. *Am. Nat.* 95:137–45

Ivey GN. 1987. Boundary mixing in a rotating stratified fluid. *J. Fluid Mech.* 183:25–44

Jester R, Lefebvre K, Langlois G, Vigilant V, Baugh K, Silver MW. 2009. A shift in the dominant toxin-producing algal species in central California alter phycotoxins in food webs. *Harmful Algae* 8:291–98

Johnston TMS, Cheriton OM, Pennington JT, Chavez FP. 2009. Thin phytoplankton layer formation at eddies, filaments, and fronts in a coastal upwelling zone. *Deep-Sea Res. Part II* 56:246–59

Johnston TMS, Rudnick DL. 2009. Observations of the transition layer. *J. Phys. Oceanogr.* 39:780–97

Kamykowski D, Reed RE, Kirkpatrick GJ. 1992. Comparison of sinking velocity, swimming velocity, rotation, and path characteristics among six marine dinoflagellate species. *Mar. Biol.* 113:319–28

Kamykowski D, Yamazaki H. 1997. A study of metabolism-influenced orientation in the diel vertical migration of marine dinoflagellates. *Limnol. Oceanogr.* 42:1189–202

Karp-Boss L, Boss E, Jumars PA. 2000. Motion of dinoflagellates in a simple shear flow. *Limnol. Oceanogr.* 45:1594–602

Kasai A, Kurikawa Y, Ueno M, Robert D, Yamashita Y. 2010. Salt-wedge intrusion of seawater and its implication for phytoplankton dynamics in the Yura Estuary, Japan. *Estuar. Coast. Shelf Sci.* 86:408–14

Kessler JO. 1985. Hydrodynamic focusing of motile algal cells. *Nature* 313:218–20

Koukaras K, Nikolaidis G. 2004. Dinophysis blooms in Greek coastal waters (Thermaikos Gulf, NW Aegean Sea). *J. Plankton Res.* 26:445–57

Kudela RM, Seeyave S, Cochlan WP. 2010. The role of nutrients in regulation and promotion of harmful algal blooms in upwelling systems. *Prog. Oceanogr.* 85:122–35

Kundu PK, Cohen IM. 2004. *Fluid Mechanics*. San Diego: Elsevier. 3rd ed.

Lasker R. 1975. Field criteria for survival of anchovy larvae: relation between inshore chlorophyll maximum layers and successful first feeding. *Fish. Bull.* 73:453–62

Lebert M, Häder DP. 1996. How *Euglena* tells up from down. *Nature* 379:590

Lévy M. 2008. The modulation of biological production by oceanic mesoscale turbulence. In *Transport and Mixing in Geophysical Flows*, ed. JB Weiss, A Provenzale, pp. 219–261. Lect. Notes Phys. 744. Berlin: Springer-Verlag

MacIntyre JG, Cullen JJ, Cembella AD. 1997. Vertical migration, nutrition and toxicity in the dinoflagellate *Alexandrium tamarense*. *Mar. Ecol. Prog. Ser.* 148:201–16

MacKinnon JA, Gregg MC. 2003. Mixing on the late-summer New England shelf—solibores, shear, and stratification. *J. Phys. Oceanogr.* 33:1476–92

Marcos, Seymour J, Luhar M, Durham WM, Mitchell JG, et al. 2011. Microbial alignment in flow changes ocean light climate. *Proc. Natl. Acad. Sci. USA* 108:3860–64

McCarren J, Brahamsha B. 2009. Swimming motility mutants of marine *Synechococcus* affected in production and locations of the S-layer protein swmA. *J. Bacteriol.* 191:1111–14

McManus MA, Alldredge AL, Barnard AH, Boss E, Case JF, et al. 2003. Characteristics, distribution and persistence of thin layers over a 48 hour period. *Mar. Ecol. Prog. Ser.* 261:1–19

McManus MA, Kudela RM, Silver MW, Steward GF, Donaghay PL, Sullivan JM. 2008. Cryptic blooms: Are thin layers the missing connection? *Estuar. Coasts* 31:396–401

McPhee-Shaw E. 2006. Boundary-interior exchange: reviewing the idea that internal-wave mixing enhances lateral dispersal near continental margins. *Deep-Sea Res. Part II* 53:42–59

Menden-Deuer S. 2008. Spatial and temporal characteristics of plankton-rich layers in a shallow, temperate fjord. *Mar. Ecol. Prog. Ser.* 355:21–30

Menden-Deuer S, Fredrickson K. 2010. Structure-dependent, protistan grazing and its implication for the formation, maintenance and decline of plankton patches. *Mar. Ecol. Prog. Ser.* 420:57–71

Menden-Deuer S, Grünbaum D. 2006. Individual foraging behaviors and population distributions of a planktonic predator aggregating to plankton thin layers. *Limnol. Oceanogr.* 51:109–16

Mitchell JG, Yamazaki H, Seuront L, Wolk F, Li H. 2008. Phytoplankton patch patterns: seascape anatomy in a turbulent ocean. *J. Mar. Syst.* 69:247–53

Moline MA, Benoit-Bird KJ, Robbins IC, Schroth-Miller M, Waluk CM, Zelenke B. 2010. Integrated measurements of acoustical and optical thin layers II: horizontal length scales. *Cont. Shelf Res.* 30:29–38

Mullin MM, Brooks ER. 1976. Some consequences of distributional heterogeneity of phytoplankton and zooplankton. *Limnol. Oceanogr.* 21:784–96

Nielsen TG, Kiorboe T, Bjornsen PK. 1990. Effects of a *Chrysochromulina polylepis* subsurface bloom on the planktonic community. *Mar. Ecol. Prog. Ser.* 62:21–35

Nixon SW. 1995. Coastal marine eutrophication: a definition, social causes, and future concerns. *Ophelia* 41:199–219

Osborn TR. 1998. Finestructure, microstructure, and thin layers. *Oceanography* 11:36–43

Paine RT. 1966. Food web complexity and species diversity. *Am. Nat.* 100:65–75

Park MG, Cooney SK, Kim JS, Coats DW. 2002. Effects of parasitism on diel vertical migration, phototaxis/geotaxis, and swimming speed of the bloom-forming dinoflagellate *Akashiwo sanguinea*. *Aquat. Microb. Ecol.* 29:11–18

Pedersen F. 1994. The oceanographic and biological tidal cycle succession in shallow sea fronts in the North Sea and the English Channel. *Estuar. Coast. Shelf Sci.* 38:249–69

Phillips OM, Shyu J, Salmun H. 1986. An experiment on boundary mixing: mean circulation and transport rates. *J. Fluid Mech.* 173:473–99

Polin M, Tuval I, Drescher K, Gollub JP, Goldstein RE. 2009. *Chlamydomonas* swims with two "gears" in a eukaryotic version of run-and-tumble locomotion. *Science* 325:487–90

Prairie JC, Franks PJS, Jaffe JS. 2010. Cryptic peaks: invisible vertical structure in fluorescent particles revealed using a planar laser imaging fluorometer. *Limnol. Oceanogr.* 55:1943–58

Prairie JC, Franks PJS, Jaffe JS, Doubell MJ, Yamazaki H. 2011. Physical and biological controls of vertical gradients in phytoplankton. *Limnol. Oceanogr. Fluids Environ.* 1:75–90

Preston MD, Pitchford JW, Wood AJ. 2010. Evolutionary optimality in stochastic search problems. *J. R. Soc. Interface* 7:1301–10

Ralston DK, McGillicuddy DJ, Townsend DW. 2007. Asynchronous vertical migration and bimodal distribution of motile phytoplankton. *J. Plankton Res.* 29:803–21

Richardson TL, Cullen JJ, Kelley DE, Lewis MR. 1998. Potential contributions of vertically migrating *Rhizosolenia* to nutrient cycling and new production in the open ocean. *J. Plankton Res.* 20:219–41

Rines JEB, Donaghay PL, Dekshenieks MM, Sullivan JM, Twardowski MS. 2002. Thin layers and camouflage: hidden *Pseudo-nitzschia* spp. (Bacillariophyceae) populations in a fjord in the San Juan Islands, Washington, USA. *Mar. Ecol. Prog. Ser.* 225:123–37

Rines JEB, McFarland MN, Donaghay PL, Sullivan JM. 2010. Thin layers and species-specific characterization of the phytoplankton community in Monterey Bay, California, USA. *Cont. Shelf Res.* 30:66–80

Roberts AM, Deacon FM. 2002. Gravitaxis in motile micro-organisms: the role of fore-aft body asymmetry. *J. Fluid Mech.* 452:405–23

Ross ON, Sharples J. 2004. Recipe for 1-D Lagrangian particle tracking models in space-varying diffusivity. *Limnol. Oceanogr. Methods* 2:289–302

Ryan JP, McManus MA, Paduan JD, Chavez FP. 2008. Phytoplankton thin layers caused by shear in frontal zones of a coastal upwelling system. *Mar. Ecol. Prog. Ser.* 354:21–34

Ryan JP, McManus MA, Sullivan JM. 2010. Interacting physical, chemical and biological forcing of phytoplankton thin-layer variability in Monterey Bay, California. *Cont. Shelf Res.* 30:7–16

Sellner KG, Doucette GJ, Kirkpatrick GJ. 2003. Harmful algal blooms: causes, impacts and detection. *J. Ind. Microbiol. Biotechnol.* 30:383–406

Seymour JR, Marcos, Stocker R. 2009. Resource patch formation and exploitation throughout the marine microbial food web. *Am. Nat.* 173:15–29

Simpson JH, Tett PB, Argoteespinoza ML, Edwards A, Jones KJ, Savidge G. 1982. Mixing and phytoplankton growth around an island in a stratified sea. *Cont. Shelf Res.* 1:15–31

Smayda TJ. 1997. Harmful algal blooms: their ecophysiology and general relevance to phytoplankton blooms in the sea. *Limnol. Oceanogr.* 42:1137–53

Stacey MT, McManus MA, Steinbuck JV. 2007. Convergences and divergences and thin layer formation and maintenance. *Limnol. Oceanogr.* 52:1523–32

Steele JH. 1974. Spatial heterogeneity and population stability. *Nature* 248:83

Steinbuck JV, Genin A, Monismith SG, Koseff JR, Holzman R, Labiosa RG. 2010. Turbulent mixing in fine-scale phytoplankton layers: observations and inferences of layer dynamics. *Cont. Shelf Res.* 30:442–55

Develops scaling relations for the expected layer thickness based on the competition between various convergence mechanisms and turbulent dispersion.

Applies a systematic, deductive approach to determine the mechanism responsible for layer formation, providing a template for the analysis of future field observations.

Steinbuck JV, Stacey MT, McManus MA, Cheriton OM, Ryan JP. 2009. Observations of turbulent mixing in a phytoplankton thin layer: implications for formation, maintenance, and breakdown. *Limnol. Oceanogr.* 54:1353–68

Stocker R, Imberger J. 2003. Horizontal transport and dispersion in the surface layer of a medium-sized lake. *Limnol. Oceanogr.* 48:971–82

Strickland JDH. 1968. A comparison of profiles of nutrient and chlorophyll concentrations taken from discrete depths and by continuous recording. *Limnol. Oceanogr.* 13:388–91

Sullivan JM, Donaghay PL, Rines JEB. 2010a. Coastal thin layer dynamics: consequences to biology and optics. *Cont. Shelf Res.* 30:50–65

Sullivan JM, Van Holliday D, McFarland M, McManus MA, Cheriton OM, et al. 2010b. Layered organization in the coastal ocean: an introduction to planktonic thin layers and the LOCO project. *Cont. Shelf Res.* 30:1–6

Tiselius P. 1992. Behavior of *Acartia tonsa* in patchy food environments. *Limnol. Oceanogr.* 37:1640–51

Tiselius P, Jonsson PR, Verity PG. 1993. A model evaluation of the impact of food patchiness on foraging strategy and predation risk in zooplankton. *Bull. Mar. Sci.* 53:247–64

Townsend DW, Bennett SL, Thomas MA. 2005. Diel vertical distributions of the red tide dinoflagellate *Alexandrium fundyense* in the Gulf of Maine. *Deep-Sea Res. Part II* 52:2593–602

Turner JT, Tester PA. 1997. Toxic marine phytoplankton, zooplankton grazers, and pelagic food webs. *Limnol. Oceanogr.* 42:1203–14

Twardowski MS, Sullivan JM, Donaghay PL, Zaneveld JRV. 1999. Microscale quantification of the absorption by dissolved and particulate material in coastal waters with an ac-9. *J. Atmos. Ocean. Technol.* 16:691–707

Tyler MA, Seliger HH. 1978. Annual subsurface transport of a red tide dinoflagellate to its bloom area: water circulation patterns and organism distributions in Chesapeake Bay. *Limnol. Oceanogr.* 23:227–46

Vanierland ET, Peperzak L. 1984. Separation of marine seston and density determination of marine diatoms by density gradient centrifugation. *J. Plankton Res.* 6:29–44

Villareal TA, Carpenter EJ. 2003. Buoyancy regulation and the potential for vertical migration in the oceanic cyanobacterium *Trichodesmium*. *Microb. Ecol.* 45:1–10

Visser AW. 1997. Using random walk models to simulate the vertical distribution of particles in a turbulent water column. *Mar. Ecol. Prog. Ser.* 158:275–81

Walsby AE. 1972. Structure and function of gas vacuoles. *Bacteriol. Rev.* 36:1–32

Waterbury JB, Willey JM, Franks DG, Valois FW, Watson SW. 1985. A cyanobacterium capable of swimming motility. *Science* 230:74–76

Waters RL, Mitchell JG, Seymour J. 2003. Geostatistical characterisation of centimetre-scale spatial structure of in vivo fluorescence. *Mar. Ecol. Prog. Ser.* 251:49–58

White AE, Spitz YH, Letelier RM. 2006. Modeling carbohydrate ballasting by *Trichodesmium* spp. *Mar. Ecol. Prog. Ser.* 323:35–45

Woodson CB, Webster DR, Weissburg MJ, Yen J. 2005. Response of copepods to physical gradients associated with structure in the ocean. *Limnol. Oceanogr.* 50:1552–64

Woodson CB, Webster DR, Weissburg MJ, Yen J. 2007. Cue hierarchy and foraging in calanoid copepods: ecological implications of oceanographic structure. *Mar. Ecol. Prog. Ser.* 330:163–77

Tests the hypothesis that thin layers can form by convergent swimming, by inferring swimming speeds from field measurements.

Provides the first published report of thin phytoplankton layers, presciently noting that thin layers limit our ability to measure phytoplankton abundance with traditional techniques.

**Annual Review of
Marine Science**

Volume 4, 2012

Contents

Errata

An online log of corrections to *Annual Review of Marine Science* articles may be found at
http://marine.annualreviews.org/errata.shtml